

1   **Ammonium-adduct chemical ionization to investigate  
2   anthropogenic oxygenated gas-phase organic compounds in  
3   urban air**

4  
5   Peeyush Khare<sup>1,1</sup>, Jordan E. Krechmer<sup>2</sup>, Jo Ellen Machesky<sup>1</sup>, Tori Hass-Mitchell<sup>1</sup>, Cong Cao<sup>3</sup>,  
6   Junqi Wang<sup>1</sup>, Francesca Majluf<sup>2,\*\*\*</sup>, Felipe Lopez-Hilfiker<sup>4</sup>, Sonja Malek<sup>1</sup>, Will Wang<sup>1</sup>, Karl  
7   Seltzer<sup>5</sup>, Havaula O.T. Pye<sup>6</sup>, Roisin Commane<sup>7</sup>, Brian C. McDonald<sup>8</sup>, Ricardo Toledo-Crow<sup>9</sup>, John  
8   E. Mak<sup>3</sup>, Drew R. Gentner<sup>1,10</sup>

9  
10   <sup>1</sup>Department of Chemical and Environmental Engineering, Yale University, New Haven CT-06511 USA  
11   <sup>2</sup>Aerodyne Research Inc. Billerica MA- 02181 USA

12   <sup>3</sup>School of Marine and Atmospheric Science, Stony Brook University, Stony Brook NY-11794 USA

13   <sup>4</sup>Tofwerk AG, CH-3600 Thun, Switzerland

14   <sup>5</sup>Office of Air and Radiation, Environmental Protection Agency, Research Triangle Park, NC-27711 USA

15   <sup>6</sup>Office of Research and Development, Environmental Protection Agency, Research Triangle Park, NC-  
16   27711 USA

17   <sup>7</sup>Department of Earth and Environmental Sciences, Lamont-Doherty Earth Observatory, Columbia  
18   University, New York, NY-10027 USA

19   <sup>8</sup>Chemical Sciences Laboratory, National Oceanic and Atmospheric Administration, Boulder CO- USA

20   <sup>9</sup>Advanced Science Research Center, City University of New York, New York, NY-10031 USA

21   <sup>10</sup>School of the Environment, Yale University, New Haven CT-06511 USA

22   <sup>1</sup>now at: Laboratory of Atmospheric Chemistry, Paul Scherrer Institute, Villigen AG-5232 Switzerland

23   <sup>\*\*</sup> now at: Franklin W. Olin College of Engineering (fmajluf@olin.edu, (781) 292-2300).

24

25   Corresponding authors: Jordan E. Krechmer (krechmer@ aerodyne.com) and Drew R. Gentner  
26   (drew.gentner@yale.edu)

27

28   **Abstract**

29   Volatile chemical products (VCPs) and other non-combustion-related sources have  
30   become important for urban air quality, and bottom-up calculations report emissions of a  
31   variety of functionalized compounds that remain understudied and uncertain in emissions  
32   estimates. Using a new instrumental configuration, we present online measurements of  
33   oxygenated **VCPs** in a U.S. megacity over a 10-day wintertime  
34   sampling period, when biogenic sources and photochemistry were less active.

35   Measurements were conducted at a rooftop observatory in upper Manhattan, New York  
36   City, USA using a Vocus chemical ionization time-of-flight mass spectrometer with  
37   ammonium ( $\text{NH}_4^+$ ) as the reagent ion operating at 1 Hz. The range of observations  
38   spanned volatile, intermediate-volatility, and semi-volatile organic compounds with  
39   targeted analyses of ~150 ions whose likely assignments included a range of  
40   functionalized compound classes such as glycols, glycol ethers, acetates, acids, alcohols,  
41   acrylates, esters, ethanolamines, and ketones that are found in various consumer,  
42   commercial, and industrial products. Their concentrations varied as a function of wind  
43   direction with enhancements over the highly-populated areas of the Bronx, Manhattan,

44 and parts of New Jersey, and included abundant concentrations of acetates, acrylates,  
45 ethylene glycol, and other commonly-used oxygenated compounds. The results provide  
46 top-down constraints on wintertime emissions of these oxygenated/functionalized  
47 compounds with ratios to common anthropogenic marker compounds, and  
48 ~~compares~~comparisons of their relative abundances to two regionally-resolved emissions  
49 inventories used in urban air quality models.

50

51 **Keywords:** Volatile chemical products, non-combustion-related emissions, personal care  
52 products, solvents, glycol ethers, VOCs, IVOCs, SVOCs, urban air quality, New York  
53 City, LISTOS, ~~AEROMMA~~

54

## 55 1. Introduction

56 Non-combustion-related sources are increasingly important contributors of anthropogenic  
57 emissions in developed regions and megacities with implications for tropospheric ozone  
58 and secondary organic aerosols (SOA) (Coggon et al., 2021; Khare and Gentner, 2018;  
59 Mcdonald et al., 2018; Pennington et al., 2021; Shah et al., 2020). These sources include  
60 volatile chemical products (VCPs), asphalt, and other products/materials that emit  
61 volatile-, intermediate- and semi-volatile organic compounds (VOCs, IVOCs, SVOCs),  
62 which contribute to the atmospheric burden of reactive organic carbon (ROC) (Heald and  
63 Kroll, 2020). Emissions occur over timescales ranging from minutes to several days and  
64 up to years in some cases (Khare and Gentner, 2018). Compounds from VCPs are diverse  
65 in terms of chemical composition and depend on application methods and uses of  
66 different products and materials. Examples of compound classes found in consumer and  
67 commercial products include hydrocarbons, acetates, alcohols, glycols, glycol ethers,  
68 fatty acid methyl esters, aldehydes, siloxanes, ethanolamines, phthalates and acids (Bi et  
69 al., 2015; Even et al., 2019, 2020; Khare and Gentner, 2018; Mcdonald et al., 2018).

70

71 A subset of compounds from these classes have been investigated in indoor environments  
72 for sources like building components (e.g. paints), household products (e.g. cleaners,  
73 insecticides, fragrances), and for some from polymer-based items such as textiles and  
74 toys (Bi et al., 2015; Even et al., 2020; Harb et al., 2020; Liang et al., 2015; Noguchi and  
75 Yamasaki, 2020; Shi et al., 2018; Singer et al., 2006). Emissions are often dependent on  
76 volatilization and thus can exhibit dependence on temperature (Khare et al., 2020).  
77 However, other environmental factors such as relative humidity can sustain or enhance  
78 indoor air concentrations of a wide range of compounds including alcohols, glycols and  
79 glycol ethers for months after application of paints (Choi et al., 2010b; Markowicz and  
80 Larsson, 2015). Similarly, mono-ethanolamines from degreasers and oxygenated third-

81 hand cigarette smoke compounds have also been shown to off-gas and persist in indoor  
82 air for days or more after application or use (Schwarz et al., 2017; Sheu et al., 2020).

83

84 ~~Non-combustion related emissions of ROC can present health risks through direct~~  
85 ~~exposure in both indoor and outdoor environments and via SOA and ozone production~~  
86 ~~(Bornehag et al., 2005; Choi et al., 2010a; Destaillats et al., 2006; Masuck et al., 2011;~~  
87 ~~Pye et al., 2021; Qin et al., 2020; Wensing et al., 2005). These health impacts will be~~  
88 ~~modulated by the rate~~ at which indoor emissions of ROC are transferred outdoors (Sheu  
89 et al., 2021), but indoor sinks are uncertain and have often been neglected in emissions  
90 inventory development for VCPs until recently (McDonald et al., 2018; Seltzer et al.,  
91 2021b). Information on indoor and outdoor concentrations of many ROC compounds is  
92 limited due to the historical focus on more volatile hydrocarbons and small oxygenated  
93 compounds (e.g. methanol, isopropanol, acetone) and shorter timescales of solvent  
94 evaporation (e.g. <1 day). In comparison, emissions of intermediate- and semi-volatile  
95 compounds (ISVOCs; including higher molecular weight oxygenates) and some  
96 chemical functionalities (e.g. glycol ethers) are poorly constrained, owing to  
97 instrumentation challenges and/or long emission timescales (Khare and Gentner, 2018).

98

99 Single-ring aromatic VOCs (e.g. benzene, toluene, ethylbenzene, xylenes) have  
100 historically been well-known contributors to urban ozone and SOA production (Henze et  
101 al., 2008; Venecek et al., 2018). On this basis, regulatory policies drove a shift towards  
102 oxygenates to replace these aromatics and other unsaturated hydrocarbons as solvents  
103 (Council of the European Union, 1999), which has influenced the ambient composition  
104 of oxygenated volatile organic compounds (OVOCs) (Venecek et al., 2018). Recent top-  
105 down measurements have revealed large upward fluxes of OVOCs in urban environments  
106 that double the previous urban anthropogenic emission estimates (Karl et al., 2018).

107 Other studies have found substantial VCP-related emissions (e.g.

108 Decamethylcyclopentasiloxane or D5) to outdoor environments in several large cities  
109 such as Boulder, CO; New York, NY; Los Angeles, CA and Toronto, Canada (Coggon et  
110 al., 2018, 2021; Gkatzelis et al., 2021b, 2021a; Khare and Gentner, 2018; McDonald et  
111 al., 2018; McLachlan et al., 2010). Offline laboratory experiments with select VCP-  
112 related precursors have also shown significant SOA yields from oxygenated aromatic  
113 precursors (Charan et al., 2020; Humes et al., 2022). Furthermore, bottom-up estimates  
114 suggest that 75-90% of the non-combustion emissions are constituted by functionalized  
115 species while only the remaining 10-25% are hydrocarbons (Khare and Gentner, 2018;  
116 McDonald et al., 2018).

117

Field Code Changed

118 Non-combustion-related emissions of ROC can present health risks through direct  
119 exposure in both indoor and outdoor environments and via SOA and ozone production  
120 (Bornehag et al., 2005; Choi et al., 2010a; Destaillats et al., 2006; Masuck et al., 2011;  
121 Pye et al., 2021; Qin et al., 2020; Wensing et al., 2005). These health impacts will be  
122 modulated by the air exchange rates at which indoor emissions of ROC are transferred  
123 outdoors (Sheu et al., 2021), but indoor sinks are uncertain and have often been neglected  
124 in emissions inventory development for VCP-related sources until recently (McDonald et  
125 al., 2018; Seltzer et al., 2021b). Information on indoor and outdoor concentrations of  
126 many ROC compounds is limited due to the historical focus on more volatile  
127 hydrocarbons and small oxygenated compounds (e.g. methanol, isopropanol, acetone)  
128 and shorter timescales of solvent evaporation (e.g. <1 day). In comparison, emissions of  
129 intermediate- and semi-volatile compounds (ISVOCs; including higher molecular weight  
130 oxygenates) and some chemical functionalities (e.g. glycol ethers) are poorly constrained,  
131 owing to instrumentation challenges and/or long emission timescales (Khare and  
132 Gentner, 2018).

133

134 ~~To improve observational constraints on the abundances of widely used oxygenated~~  
135 ~~VCPs that are expected to influence urban air quality, but are uncertain in emissions~~  
136 ~~inventories, we employed a Vocus chemical ionization time-of-flight mass spectrometer~~  
137 ~~(Vocus CI-ToF) using ammonium ( $\text{NH}_4^+$ ) as a chemical reagent ion to increase~~  
138 ~~sensitivity to compound types that have traditionally provided measurement challenges.~~  
139 ~~Specifically, we: (a) evaluated the performance of the CI-ToF for a diverse array of~~  
140 ~~oxygenated VCPs and compare ambient observations between  $\text{NH}_4^+$  and  $\text{H}_3\text{O}^+$  reagent~~  
141 ~~ions; (b) examined ambient abundances of a subset of oxygenated gas phase organics~~  
142 ~~related to VCP emissions and their dynamic atmospheric concentrations in New York~~  
143 ~~City (NYC) over a 10-day winter period with reduced biogenic emissions and secondary~~  
144 ~~OVOC production; (c) determined their ambient concentration ratios and covariances~~  
145 ~~with major tracer compounds; and (d) compared ambient observations against two~~  
146 ~~regionally resolved emissions inventories to provide top down constraints on the relative~~  
147 ~~emissions of major oxygenated VCPs that influence urban air quality. The findings of this~~  
148 ~~work highlight the diversity of functionalized organic species emitted from VCPs with~~  
149 ~~comparisons against inventories that inform our understanding of VCP composition and~~  
150 ~~emission pathways, and thus improve urban air quality models and policy.~~

151

## 152 **2. Materials and methods**

153 ~~The sampling site was located at the Rooftop Observatory at the Advanced Science~~  
154 ~~Research Center of the City University of New York (CUNY ASRC, 85 St.~~

155 To improve observational constraints on the abundances of widely-used oxygenated  
156 VCPs that are expected to influence urban air quality, but are uncertain in emissions  
157 inventories, we employed a Vocus chemical ionization time-of-flight mass spectrometer  
158 (Vocus CI-ToF MS) using ammonium ( $\text{NH}_4^+$ ) as a chemical reagent ion to increase  
159 sensitivity to compound types that have traditionally provided measurement challenges  
160 with other well-known techniques such as iodide (I<sup>-</sup>)-CIMS and proton-transfer-reaction  
161 (PTR)-MS. These techniques have been frequently used in atmospheric studies with both  
162 advantages and limitations. While I-CIMS has better sensitivity toward highly  
163 functionalized extremely low volatility organic compounds (ELVOCs) and also halogens  
164 (Robinson et al., 2022; Slusher et al., 2004; Thornton et al., 2010), PTR-MS can detect  
165 relatively lighter functionalized species and olefinic/aromatic hydrocarbons, however  
166 with highly reduced sensitivity toward certain compound classes e.g. alcohols, esters,  
167 glycols etc. due to large fragmentation losses (Gkatzelis et al., 2021a). The ability of  
168  $\text{NH}_4^+$  adduct to ionize functionalized organic compounds as well as less oxygenated  
169 organic precursors with negligible fragmentation across volatile to semi-volatile species  
170 is a key advantage (Canaval et al., 2019; Zaytsev et al., 2019b). Furthermore, it operates  
171 at relatively lower pressure (1-5 mbar) than (I<sup>-</sup>)-CIMS, which could facilitate faster  
172 switching with PTR for quantitation of less oxygenated precursor species.

173

174 Specifically, using this technique, we: (a) evaluated the performance of the CI-ToF for a  
175 diverse array of oxygenated VCPs and compare ambient observations between  $\text{NH}_4^+$  and  
176  $\text{H}_3\text{O}^+$  reagent ions; (b) examined ambient abundances of a subset of oxygenated gas-  
177 phase organics related to VCP-related emissions and their dynamic atmospheric  
178 concentrations in New York City (NYC) over a 10-day winter period with reduced  
179 biogenic emissions and secondary OVOC production; (c) determined their ambient  
180 concentration ratios and covariances with major tracer compounds; and (d) compared  
181 ambient observations against two regionally-resolved emissions inventories (including all  
182 anthropogenic sources) to provide top-down constraints on the relative emissions of a  
183 range of oxygenated compounds that may influence urban air quality. The findings of this  
184 work highlight the diversity of functionalized organic species emitted from VCPs with  
185 comparisons against inventories that inform our understanding of VCP composition and  
186 emission pathways, and thus improve urban air quality models and policy.

187

## 188 **2. Materials and methods**

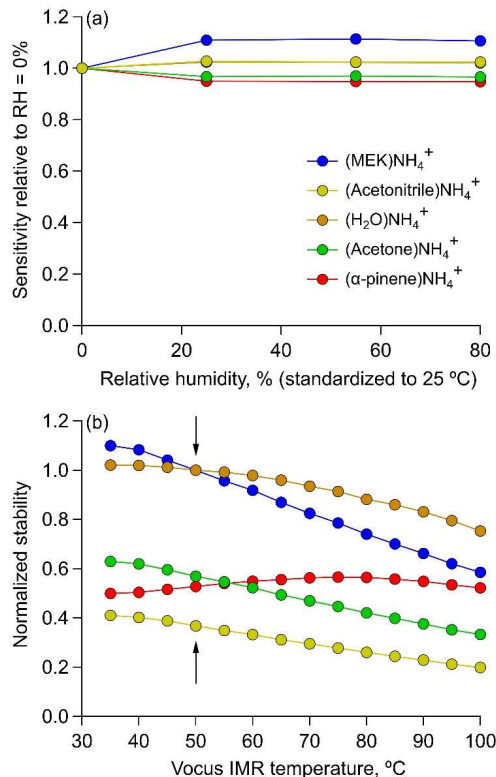
189 The sampling site was located at the Rooftop Observatory at the Advanced Science  
190 Research Center of the City University of New York (CUNY ASRC, 85 St. Nicholas  
191 Terrace) in Upper Manhattan (Figures S1-2), which is the location of the Manhattan  
192 ground site for the upcoming AEROMMA research campaign (Warneke et al., n.d.).

193 The ASRC is built on top of a hill 30 m above the mean sea level whose surface is  
194 naturally elevated above the surrounding landscape. The observatory is 86 m above the  
195 mean sea level and the inlet was at 89 m with minimally obstructed views to the  
196 northwest and east towards the Bronx and Harlem, as well as to the south along the island  
197 of Manhattan.

198

199

200 Gas-phase VOCs and I/SVOCs were measured using a Vocus CI-ToF with a NH<sub>4</sub><sup>+</sup>  
201 reagent ion source (Krechmer et al., 2018), which had a higher sensitivity than most  
202 previous state-of-the-art chemical ionization-ToF instruments (without focusing) by a  
203 factor of 20 due to the quadrupole-based ion focusing, a mass resolving power of ~10,000  
204 m/Δm, and was quantitatively independent of ambient humidity changes (Figure  
205 1a)(Figure 1a) (Holzinger et al., 2019). The Vocus CI-TOF sampled at a frequency of 1  
206 Hz continuously throughout the 10-day period from 21st to 31st January 2020. NH<sub>4</sub><sup>+</sup>  
207 ionization coupled with high frequency online mass spectrometry enables measurements  
208 of functionalized compounds emitted from diverse, distributed sources in around New  
209 York City. **Ammonium**NH<sub>4</sub><sup>+</sup> has a long history of use as a positive-ion reagent gas in  
210 chemical ionization mass spectrometry, but has only recently been applied to the study of  
211 atmospheric chemistry with time-of-flight mass spectrometers (Canaval et al., 2019;  
212 Westmore and Alauddin, 1986; Zaytsev et al., 2019b, 2019a). The NH<sub>4</sub><sup>+</sup> reagent ion  
213 forms clusters effectively with polarizable molecules, providing mostly softly ionized  
214 NH<sub>4</sub><sup>+</sup>-molecule adducts, though some protonation, charge transfer, and fragmentation can  
215 occur as alternate ionization pathways (Canaval et al., 2019). It has previously been  
216 applied in laboratory studies in different configurations than the instrument described  
217 here (Canaval et al., 2019; Zaytsev et al., 2019b), and to our knowledge this is the first  
218 published atmospheric field measurement with NH<sub>4</sub><sup>+</sup>ionization.



219  
 220  
 221 **Figure 1: Vocus CI-ToF performance with low-pressure NH<sub>4</sub><sup>+</sup> ionization as a**  
 222 **function of atmospheric conditions and instrument parameters. (a) Minimal effects**  
 223 **of relative humidity (RH) on Vocus CI-ToF quantification for several major**  
 224 **compounds using the NH<sub>4</sub><sup>+</sup> Vocus CI-ToF (b) Ion-adduct stability as a function of**  
 225 **temperature in the focusing Ion Molecule Reaction (fIMR) region, with ambient**  
 226 **measurements made at 50 °C in this study.**

227  
 228  
 229 NH<sub>4</sub><sup>+</sup> selectively ionizes functionalized species including ones that have generally been  
 230 difficult to measure using proton-transfer reaction ionization due to excess fragmentation  
 231 (e.g. glycols) or low proton affinities (Karl et al., 2018). However, it excludes non-polar  
 232 hydrocarbons and is not intended to examine emissions from hydrocarbon-dominated  
 233 non-combustion sources (e.g. mineral spirits, petroleum distillates).

235 To produce  $\text{NH}_4^+$  reagent ions in the Vocus focusing ion molecule reactor (fIMR), 20  
236 sccm of water ( $\text{H}_2\text{O}$ ) vapor and 1 sccm of vapor from a 1% ammonium hydroxide in  $\text{H}_2\text{O}$   
237 solution were injected into the discharge ion source. In addition to forming  $(\text{NH}_4^+) \text{H}_2\text{O}$   
238 as the primary reagent ion, the relatively large amount of water buffers the source against  
239 any changes in relative humidity, removing any quantitative humidity dependence and  
240 the need for humidity-dependent calibrations. This lack of RH-dependence is shown in  
241 Figure 1. The slight change in the sensitivity of methyl ethyl ketone (MEK) when  
242 increasing from 0% RH likely resulted from the three-body stabilizing effect of water,  
243 which enhances ion-adduct stability, thereby increasing this compound's sensitivity.  
244 Further details on RH-dependence of a wider set of organic species could be found in Xu  
245 et al (Xu et al., 2022). The Vocus axial voltage was maintained at a potential difference  
246 of 425 V and the reactor was maintained at a pressure of 3.0 mbar and temperature of 50  
247 °C (to maximize thermal stability as shown in Figure 1b), which corresponds to an E/N  
248 value of 70 Td. Additional characterization tests, including scans of the voltage  
249 differentials, are shown in Figure S3 and were used to inform our choice of instrument  
250 settings for the ambient measurements.

252

253

254 The instrument inlet was set up at the southeast corner of the observatory. 100 sccm of air  
255 was subsampled into the Vocus CI-ToF from a Fluorinated Ethylene Propylene (FEP)  
256 Teflon inlet 5 m long and with a 12.7 mm outer diameter that had a flowrate of 20 liters  
257  $\text{min}^{-1}$  resulting in a residence time of  $\sim 1$  s. Importantly for measurements of semi-volatile  
258 VCPs, no particulate filter was used on the inlet to enhance transmission of semi- and  
259 low-volatility gases (Krechmer et al., 2016; Pagonis et al., 2017).

260

261

262 The instrument background was measured every 15 minutes for 1 minute by injecting  
263 purified air generated by a Pt/Pd catalyst heated to 400 °C. Every 4 hours, diluted  
264 contents from a 14-component calibration cylinder (Apel-Riemer Environmental) were  
265 injected for 1 minute to measure and track instrument response over time (Table S1). To  
266 quantify CI-ToF signals for additional VCPs of interest, after the campaign we injected  
267 prepared quantitative standards of specific water-soluble VCPs that were observed in  
268 field measurements into the instrument from a Liquid Calibration System (LCS;  
269 TOFWERK AG) and measured the instrument response to create multi-point calibration  
270 curves. The LCS standards were then normalized using the cylinder calibrations during  
271 and after the campaign with the same tank. Although the CI-ToF used the same settings  
272 for calibrations as in the campaigns, this normalization accounted for differences in the  
273 instrument performance during and after the campaign. A table of the standard  
274 compounds along with their instrument responses can be found in Table S2.

275  
276  
277 Data were processed using Tofware version 3.2.3 (Aerodyne Research, Inc.) in the Igor  
278 Pro programming environment (Wavemetrics, Inc.). Compounds of interest were detected  
279 as NH<sub>4</sub><sup>+</sup> adducts within 2 ppm mass accuracy, but for clarity we refer to detected signals  
280 after subtracting the ammonium adduct (e.g. C<sub>3</sub>H<sub>6</sub>O instead of (NH<sub>4</sub>)C<sub>3</sub>H<sub>6</sub>O<sup>+</sup>) in the  
281 Results and Discussion section below. For this focused analysis of urban emissions, data  
282 filtering was also performed on a subset of compounds to remove the influence of  
283 biomass burning events which resulted in elevated benzene to toluene ratios during  
284 inflow of air from the less densely populated western direction. These additional  
285 contributions from biomass burning-related emissions would not be included in the  
286 inventoried emissions and would bias calculations of urban emission ratios in this study.  
287 ~~Hourly periods with large contributions from biomass burning were filtered for affected~~  
288 ~~compounds using a benzene-to-toluene ratio >2. Hourly periods with large contributions~~  
289 ~~from biomass burning were filtered for affected compounds using a benzene-to-toluene~~  
290 ~~ratio >1.8 (Figure S4), as acetonitrile was not well-correlated with benzene-to-toluene~~  
291 ~~ratios, which was a better indicator of the influence of biomass burning at the site~~  
292 ~~(Huangfu et al., 2021; Koss et al., 2018; Sheu et al., 2020).~~ Thus, elevated concentrations  
293 of oxygenated compounds coincided with inflow from the more densely populated areas  
294 of the city.  
295  
296

297 In addition to online measurements, a subset of adsorbent tube samples were also  
298 collected during ~~the~~ Winter 2020 ~~campaign~~ for offline analysis using gas chromatography  
299 electron ionization mass spectrometry (GC EI-MS) (Sheu et al., 2018) and were used  
300 here ~~to confirm where possible within the identifications in instrument capabilites and range~~  
301 ~~of oxygenated VCPs measured species to confirm the identifications of oxygenated~~  
302 ~~compounds (and their isomers) measured as molecular formulas by the online CI-TOF.~~  
303 ~~These supplemental tube samples were collected periodically during the measurement~~  
304 ~~period and their use here was intended to provide confirmational identifications of~~  
305 ~~isomers contributing to CI-TOF ion measurements, though may not be inclusive of all~~  
306 ~~possible OVOCs where compound or instrument configuration limitations exist (e.g., GC~~  
307 ~~transmission, reactivity, thermal instability, adsorbent/column configuration).~~ Additional  
308 measurements of meteorological parameters (e.g. wind speed/direction) (ATMOS 41  
309 weather station) and carbon monoxide (Picarro G2401m) were also collected at the  
310 sampling site. A co-located high-resolution proton-transfer-reaction time-of-flight mass  
311 spectrometer (Ionicon Analytik PTR-ToF 8000) from Stony Brook University also made  
312 coincident long-term measurements ~~of a smaller subset of key species~~, some of which  
313 were used to validate the performance of the CI-TOF with NH<sub>4</sub><sup>+</sup> ionization.  
314  
315

316 [Annual](#)[To accompany other anthropogenic sources in the EPA emissions inventory,](#)  
317 [annual](#) emissions from VCPs in NYC counties were estimated using VCPy.v2.0 [with a](#)  
318 [sector-wide uncertainty of 15% on average](#) (Seltzer et al., 2021, 2022). [These are](#)  
319 [discussed in subsequent sections together with contributions from other anthropogenic](#)  
320 [sources \(derived from National Emissions Inventory \(NEI\)\) as NEI+VCPy \(hereafter](#)  
321 [VCPy+\).](#) Additional NYC-resolved comparisons are made with the FIVE-VCP  
322 emissions inventory developed at the U.S. National Oceanic and Atmospheric  
323 Administration using methods described by McDonald et al. (McDonald et al., 2018) and  
324 updated for New York City in Coggon et al. [\(Coggon et al., 2021\)](#)[\(Coggon et al., 2021\)](#).  
325 A major update in the latter study was updating the VCP speciation profiles to the most  
326 recent surveys of consumer products, fragrances and architectural coatings. In VCPy, the  
327 magnitude and speciation of organic emissions are directly related to the mass of  
328 chemical products used, the composition of these products, the physiochemical properties  
329 of the chemical product constituents that govern volatilization, and the timescale  
330 available for these constituents to evaporate. The most notable updates to VCPy include  
331 the incorporation of additional product aggregations (e.g., 17 types of industrial  
332 coatings), variation in the VOC-content of products to reflect state-level area source rules  
333 relevant to the solvent sector, and the adoption of an indoor emissions pathway.

334

335

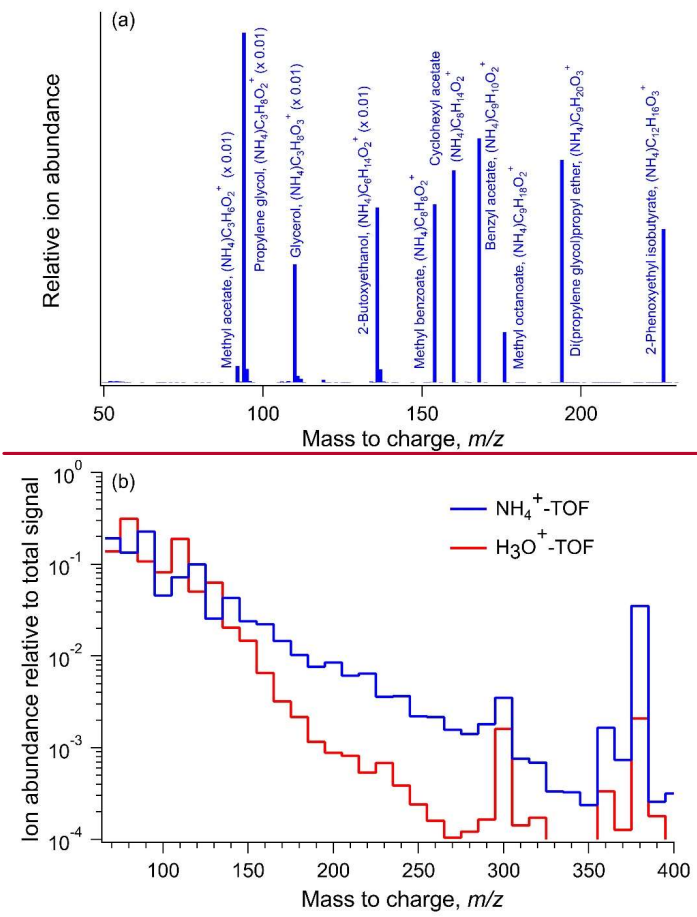
336 To facilitate calculation of VCP indoor emissions in VCPy, each product category is  
337 assigned an indoor usage fraction. All coating and industrial products are assigned a 50%  
338 indoor emission fraction, all pesticides and automotive aftermarket products are assigned  
339 a 0% indoor emission fraction, and all consumer and cleaning products are assigned a  
340 100% indoor emission fraction. The lone exception are daily use personal care products,  
341 which are assumed to have a 50% indoor emission fraction. This indoor emission  
342 assignment enables the mass transfer coefficient to vary between indoor and outdoor  
343 conditions. Typically, the mass transfer coefficient indoors is smaller than the mass  
344 transfer coefficient outdoors due to more stagnant atmospheric conditions, and the newest  
345 version of the modeling framework reflects these dynamics. Indoor product usage utilizes  
346 a mass transfer coefficient of  $5 \text{ m hr}^{-1}$ , and the remaining outdoor portion is assigned a  
347 mass transfer coefficient of  $30 \text{ m hr}^{-1}$  (Khare and Gentner, 2018; Weschler and Nazaroff,  
348 2008). More details about the framework could be found elsewhere (Seltzer et al., 2021).  
349 Annual production volumes for different chemical species used in discussion were taken  
350 from U.S. EPA's Chemical Data Reporting database (U.S. Environmental Protection  
351 Agency, Chemical Data Reporting, 2016).

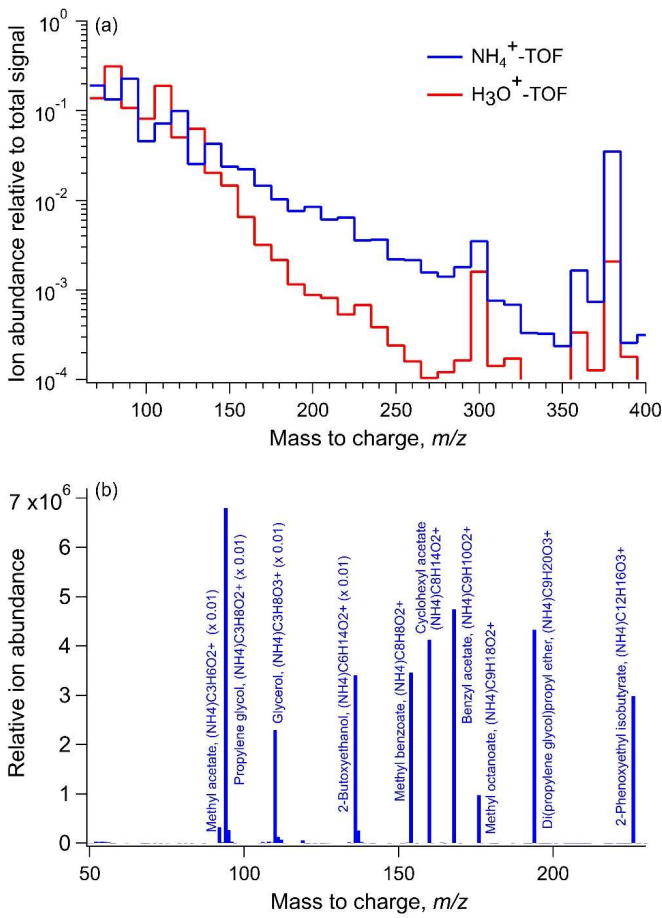
352

### 353 **3. Results and discussion**

#### 354 **3.1. Instrument response to diverse chemical functionalities**

355 Of the 1000's of ions observed in the urban ambient mass spectra (Figures 2a, [S4S5](#))  
356 during online sampling with ammonium-adduct ionization, 148 prominent ion signals  
357 were targeted for detailed analysis and assigned compound formulas representing a  
358 diverse range of chemical functionalities (Table S3). These ions were selected based on  
359 high signal-to-noise ratios ( $\geq 3.0$ ) and likely isomer contributions from [VCPs](#)[VCP](#)-related  
360 emissions. To confirm sensitivity toward these functional groups, the instrument was  
361 calibrated using 58 analytical standards that are also constituents of various  
362 consumer/commercial products. The mass spectrum of individual standards showed high  
363 parent ion-to-background signal and negligible fragmentation products (Figure 2a), ~~thus~~  
364 [simplifying](#)). [Further analysis also showed ammonium-adduct formation to be the](#)  
365 [dominant ionization pathway for these analytical standards for applied instrument settings](#)  
366 [\(Table S4\). This simplified](#) the interpretation of the soft adduct parent ions in ambient air  
367 mass spectra in contrast to higher-fragmentation-prone proton transfer reaction spectra.





369  
370 **Figure 2. (a)** Negligible parent ion fragmentation (with high signal-to-noise ratios)  
371 across diverse chemical functionalities in CI-ToF allows for measurements of  
372 understudied chemical species (examples from authentic standards shown). **(b)**  
373 Average ToF mass spectra obtained from  $\text{NH}_4^+$  and  $\text{H}_3\text{O}^+$  (i.e. PTR) ionization  
374 schemes binned over 10  $m/z$  intervals using data from the same Vocus CI-ToF at the  
375 site. The CI-ToF spectra observed greater ion signal in the approximate  
376 intermediate-volatility into the semi-volatile region (e.g.,  $\geq 160$   $m/z$ ). Note: In (b), the  
377  $\text{NH}_4^+$  and PTR signals are offset by 18 and 1  $m/z$  respectively to account for the  
378 difference in the mass of the reagent ion and the averages are from different days  
379 when the reagent ion was switched.

380

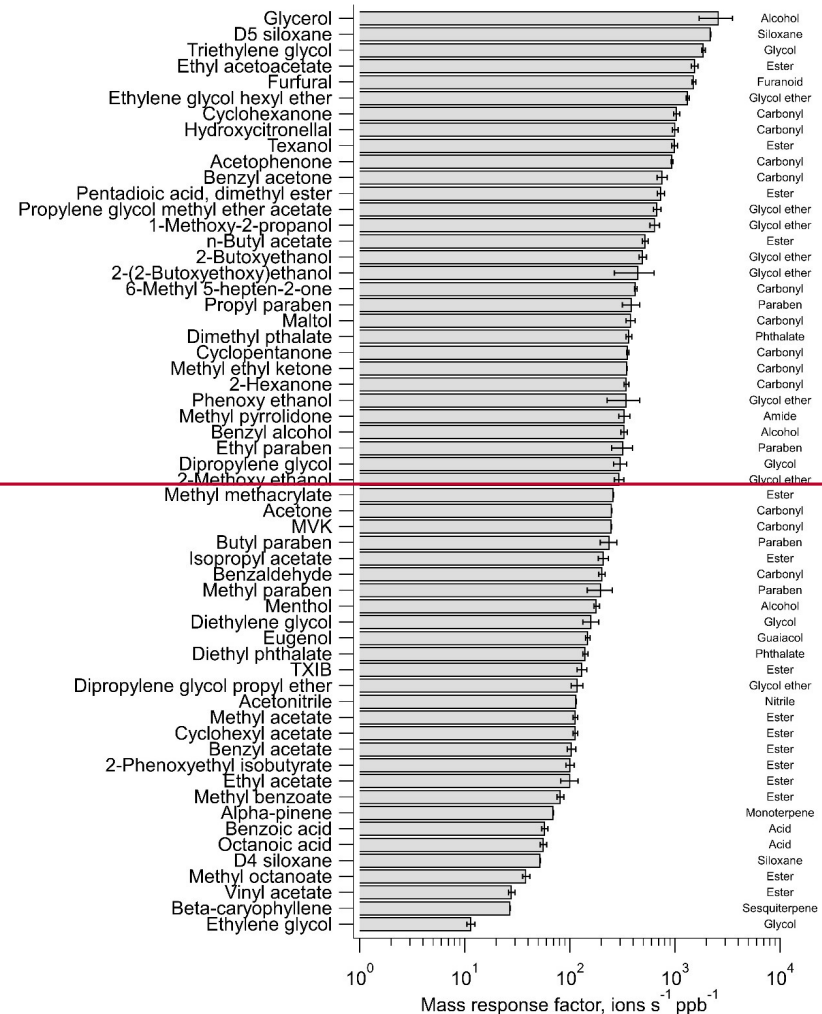
381 In laboratory tests with the authentic standards, the instrument showed the highest  
382 response factors (i.e. ions  $\text{ppb}^{-1}$ ) toward glycol ethers and ketones (Figure 3, [Table S2](#))  
383 [with detection limits below 5 parts per trillion \(ppt\) for several chemical species \(Table](#)  
384 [S5\)](#). The response factors for most aliphatic and aromatic esters were one order of  
385 magnitude smaller than glycol ethers and ketones. Standards for isomers were also run in  
386 some cases of possible different compounds contributing to the same ion signal based on  
387 multiple prominent compounds estimated in inventories or well-known VCP components.  
388 While some isomers elicited similar responses from the instrument, others produced  
389 considerably different sensitivities (Figure [S5S6](#)) (Bi et al., 2021). For 7 test cases here,  
390 the difference in response factors tended to be most pronounced in the case of isomers  
391 with small carbon numbers, e.g. ethyl acetate being 8 times higher than butyric acid,  
392 while isomers with larger carbon numbers, e.g. ethylene glycol hexyl ether (EGHE) and  
393 1,2 octanediol produced similar ion intensities. [Overall, this sensitivity analysis showed](#)  
394 [that the calculated concentrations could have significant differences \(by a factor of 0.5 to](#)  
395 [8 with a worst-case relative isomer contribution bias spanning 1:4 to 4:1\), especially for](#)  
396 [the smaller oxygenated compounds tested here, and is dependent on the relative](#)  
397 [abundance of contributing isomers due to their effect on the overall mass response factor](#)  
398 [\(Figure S6\). Hence, in each case where isomer sets were tested, the mass response factor](#)  
399 [for the ion was estimated by averaging the instrument response to individual isomers.](#)  
400 [This can still potentially cause some over- or under-estimation of ion concentrations in](#)  
401 [ambient air depending on the relative contribution of isomers to the ion, which is affected](#)  
402 [by the magnitude of emissions of individual isomers as well as their sources and sinks](#)  
403 [\(and indoor vs. outdoor emissions\). We have further constrained this uncertainty by](#)  
404 [confirming isomer identities wherever possible via offline GC-EIMS measurements using](#)  
405 [adsorbent tubes \(Table 1\).](#)

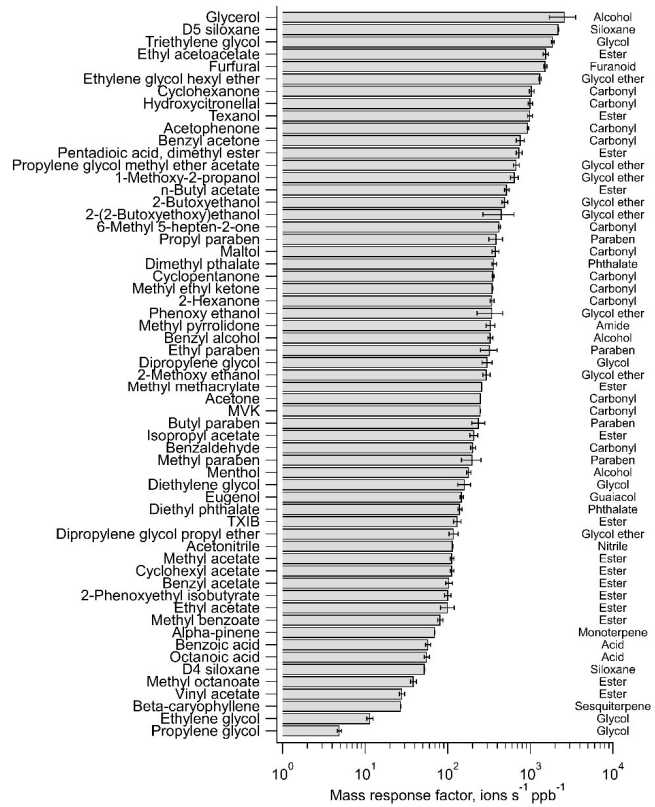
406

407 This variability in instrument response could also depend on other physiochemical  
408 properties of the analytes because some acids, e.g. hexadecanoic, fumaric, adipic and  
409 salicyclic acids, also responded poorly to calibration. This may be due to poor water  
410 solubility in some cases (e.g. adipic and hexadecanoic acid) affecting the calibration  
411 mixes, and, also the tendency of lower volatility compounds to partition to surfaces that  
412 may reduce their transmission efficiency through the LCS delivery lines and the  
413 instrument inlet thus contributing to this marked difference in instrument response  
414 between some isomers. [Sensitivity analysis showed that the calculated concentrations](#)  
415 [could have large differences \(by a factor of 0.5 to 8\) depending on the relative abundance](#)  
416 [of contributing isomers due to their effect on the overall mass response factor \(Figure](#)  
417 [S5\). Hence, in each case where isomers were tested, the mass response factor for the ion](#)  
418 [was estimated by averaging the instrument response to individual isomers. This can still](#)

419 potentially cause slight over- or under-estimation of ion concentrations in ambient air  
420 depending on the relative contribution of isomers to the ion, which is affected by the  
421 magnitude of emissions of individual isomers as well as their sources and sinks (e.g.  
422 indoor surfaces or reactions).

423  
424 The signal intensities could also be influenced by changes in environmental factors such  
425 as relative humidity that can modify the relative importance of different ionization  
426 pathways in the reaction chamber. However, systematic tests conducted with acetone,  
427 **methyl-ethyl-ketone (MEK)**, acetonitrile and  $\alpha$ -pinene found their  $\text{NH}_4^+$ -adduct signal  
428 intensities to be independent of any changes in relative humidity in the CI-ToF ionization  
429 region (Figure 1). Thus, day-to-day response factors for individual ions were comparable  
430 across the entire sampling period and did not require RH-dependent corrections.





432

433 **Figure 3.** The response of the CI-ToF with  $\text{NH}_4^+$  ionization toward select calibration  
 434 standards containing a diverse range of chemical functional groups and molecular  
 435 structures, which are listed (right) for reference, but we note the multi-functionality  
 436 of some of the compounds.

437 Additionally, the CI-ToF measurements were also validated by comparing the  
438 concentration timeseries of some of the OVOCs (i.e. acetone, methyl vinyl ketone  
439 (MVK), MEK) and monoterpenes across the entire sampling period with parallel  
440 measurements from a co-located PTR-ToF instrument. The~~While~~ the measurements  
441 largely agreed within 90%%,% validating the performance of the CI-ToF instrument  
442 (Figure S6-S7), the slight differences observed could be caused by variations in relative  
443 responses to isomers in different ionization schemes of the two instruments.  
444

445  
446 In case of ion signals that were not quantified, we have carefully considered factors such  
447 as annual usage of likely compounds, their atmospheric reactivity and ionization  
448 efficiency with the NH<sub>4</sub><sup>+</sup> adduct to inform our discussion of their formula assignments.  
449 For example, minimal ethanol ions were observed during instrument calibration  
450 suggesting limitations in its detection with NH<sub>4</sub><sup>+</sup> reagent ion. (Figure S8). Yet, C<sub>2</sub>H<sub>5</sub>OH  
451 ion signal was measured during ambient sampling. Given the densely urban sampling  
452 location, it is likely we hypothesize that this measured C<sub>2</sub>H<sub>5</sub>OH signal was dimethyl ether  
453 that is used in personal care products (propellant) and some potential use as fuel or  
454 refrigerant. It was not calibrated for and we could not confirm its abundances using  
455 another measurement in this study. However, ethanol emissions are still expected to  
456 exceed those of dimethyl ether based on the inventories. , and, instrument settings may  
457 affect its relative sensitivity between these two isomers. Similar assessments are made  
458 wherever possible in the discussion of temporal trends of uncalibrated ions.

459  
460 Vocus CI-ToF captured relatively more ion signal in the 150-350 m/z range (i.e.  
461 normalized to the total signal of the mass spectra) when compared with PTR ionization  
462 using the same instrument at the same site (Figure 2b). This was due to formation of  
463 strongly-bonded NH<sub>4</sub><sup>+</sup>-analyte adduct molecules at low collision energies that preserved  
464 large functionalized analytes. In comparison, PTR-ToF can strongly fragment certain  
465 functionalized analytes (e.g. alcohols) during proton addition rendering interpretation  
466 difficult. Hence, we are able to examine a greater diversity of volatile- to semi-volatile  
467 functionalized compounds with CI-ToF measurements that are known to be emitted from  
468 a wide range of volatile chemical products.

469  
470 **3.2 Influence of atmospheric conditions and transport on observed concentrations**  
471  
472 The concentrations of measured ions varied significantly over the 10-day sampling period  
473 influenced by changes in meteorology and dilution, as well as temporal changes in  
474 emissions. The concentrations showed clear dependence on wind velocity (4.5 m/s avg.)  
475 and direction, indicating variations in both emission rates and dispersion across different  
476 areas upwind of the site. The highest concentration signals were observed between 22/1  
477 and 25/1 when slower winds (<5 m/s) arrived from the southwest, south, and east across  
478 various parts of Manhattan leading up to the site (Figures S2, S7S9). These areas are  
479 characterized by a high population density and include a wide range of commercial  
480 activities that could contribute to the concentration enhancements. Multiple types of  
481 diverse sources of OVOCs can exist here, and in other urban areas, though current  
482 emissions inventories suggest that the inventoried target species in Table 1 are primarily  
483 emitted from VCPs in New York City with minimal or negligible contributions from  
484 other sources such as on- and non-road sources and current inventory estimates of

485 [cooking and biomass burning \(Table S6\)](#). Similarly, recent source apportionment using  
486 mobile lab measurements in NYC also attributes the majority of the signal for several of  
487 the highly emitted species observed here (e.g. acetone,  $C_2H_4O_2$ ,  $C_4H_8O$ ) to a general  
488 VCP-related source factor (that may include minor contributions from other sources)  
489 (Gkatzelis et al., 2021b).

490

491 Additional concentration spikes and smaller enhancements were observed on 27/1 with  
492 similar southwesterly winds at higher speeds. Prolonged concentration enhancements  
493 were also observed 30/1-31/1 with slower ( $<5$  m/s) winds predominantly from the east,  
494 passing over Harlem (Manhattan) after crossing the also densely-populated Bronx with  
495 varied commercial/industrial activities. Observed concentrations at the site were lowest  
496 with west-northwesterly and northwesterly winds originating from relatively less-densely  
497 populated areas, as well as periods of highest wind speeds.

498

499 Concentration trends generally overlapped across all compound classes with a few  
500 exceptions (e.g.  $C_5H_8O_2$ ), with variations in their covariances (see Sec. 3.3). This  
501 demonstrates a major role for meteorology in determining local VOC concentrations at  
502 the site, and elsewhere in NYC. Still in some cases (e.g. nitropropane, 2,5 dimethyl  
503 furan), influence of certain short-term sources such as possible local/regional wintertime  
504 biomass burning contributions were observed as temporary sharp spikes in compound  
505 abundances.

506

507 By influencing the rate of advective transport of pollutants, wind speed also directly  
508 impacts the time available for chemical species to undergo oxidation in the atmosphere.  
509 Atmospheric oxidation can be an important sink for different chemical species and also a  
510 secondary source for some OVOCs (e.g. alcohols, carbonyls) (Franco et al., 2021;  
511 Mellouki et al., 2015). Therefore, accounting for their reaction timescales is necessary in  
512 the interpretation of their relative abundances. During this sampling campaign, with a  
513 local average wind speed of  $4.5 \text{ m s}^{-1}$  (Figure S7S9), this translated to 0.5-2 hours of  
514 daytime photochemical aging for emissions within 10-30 km of the site (encompassing  
515 all of Manhattan, Brooklyn, Queens, the Bronx, and much of urban metro NYC in New  
516 Jersey) (Figure S2).

517

518 For species under consideration in this study, the rate constants for reaction with  
519 hydroxyl radicals ( $OH$ ) ranged from  $10^{-11}$  to  $10^{-13} \text{ molecule}^{-1} \text{ cm}^3 \text{ s}^{-1}$  as obtained from the  
520 OPERA model and other studies (Aschmann et al., 2001; Mansouri et al., 2018; Picquet-

Field Code Changed

521 Varrault et al., 2002; Ren et al., 2021). Given wintertime OH concentrations of  
522 approximately  $10^6$  molecules  $\text{cm}^{-3}$  in NYC (Ren et al., 2006; Schroder et al., 2018), this  
523 puts their daytime atmospheric lifetimes (i.e. e-folding times) between 1-2 days to several  
524 months with some variation ~~withacross~~ OH concentrations. For average wind speeds  
525 observed during sampling, this translated to daytime concentration losses of 10% or less  
526 for the vast majority of measured species if emitted within a distance of 10-15 kilometers  
527 of the site (Figure S8S10), which includes all of Manhattan and other densely populated  
528 areas of ~~New York City~~NYC and adjacent New Jersey (Figure S2).

529

530 Secondary production represents a major potential source of OVOCs—one that will be at  
531 a relative minimum in the wintertime conditions, but long-distance transport of OVOCs  
532 in the background air entering NYC will include significant secondary contributions, as  
533 well as some transport of primary emissions from further upwind. In the subsequent  
534 calculations of urban enhancements (Table 1) used in the emission inventory comparison  
535 (Section 3.5), these incoming background contributions are minimized by subtracting the  
536 5<sup>th</sup> percentile for each measured species to reduce the influence of non-local primary and  
537 secondary sources outside the scope of the NYC-focused inventories used here. These  
538 urban enhancement calculations (discussed further in Section 3.5) are aided by the very  
539 densely populated nature of NYC and the density of VCP-related and other  
540 anthropogenic sources. For example, recent mobile measurements that show over 95%  
541 reduction in D5 concentrations outside NYC relative to Manhattan and surrounding areas  
542 indicating minimal contributions from urban sources outside of NYC (Coggon et al.,  
543 2021). For the select VCP-related species examined in those studies and at our site, the  
544 mobile measurements (Coggon et al., 2021; Stockwell et al., 2021) in the relatively less  
545 densely-populated regions to the north and northwest of NYC show background  
546 concentrations comparable to our 5<sup>th</sup> percentile concentrations, which typically came with  
547 winds from that direction and/or periods with high wind speeds of 7-8  $\text{ms}^{-1}$  or greater  
548 (enhancing dilution) (figures 4-5, S9).

549

550 Despite wintertime conditions, local secondary production of OVOCs via atmospheric  
551 oxidation will occur (over the distances described above) with the potential for locally-  
552 produced OVOCs that could be included in the urban enhancement calculations.  
553 However, the field site's location amongst a high density of VCP-related (and other)  
554 sources and the observed OVOC enhancements occurring with winds from more densely-  
555 populated areas (Figures 4, 5, S9) supports the dominance of primary emissions in  
556 wintertime and drives the well-correlated enhancements with OVOC tracers that aids the  
557 inventory comparison. For context, Gkatzelis et al.'s (ES&T 2021b) reported that only  
558 ~20% of wintertime acetone in NYC is related to secondary production, which would

559 [include both contributions from oxidation locally and over longer distances, and the](#)  
560 [approach here subtracts the latter background contributions.](#)

561

562 For future work at the site, we note that daytime OH concentrations in NYC during  
563 summer will be higher (e.g. five times the winter values in NYC, (Ren et al., 2006)),  
564 which can affect the interpretation of source contributions to more reactive chemical  
565 species with shorter lifetimes. [and secondary production.](#) The other important daytime  
566 oxidant ozone is not likely to react significantly in the absence of non-aromatic  
567 unsaturated C=C bonds in most targeted ions in this study (de Gouw et al., 2017),  
568 especially during the winter. The [reaction rate \(k\)](#) values for nighttime oxidation with the  
569 nitrate radicals are 1 to 4 orders of magnitude smaller ( $\sim 10^{-12}$ - $10^{-15}$  molecule $^{-1}$  cm $^3$  s $^{-1}$ )  
570 with average NO<sub>3</sub> concentrations on the order of 10<sup>8</sup> molecules cm $^{-3}$  (Asaf et al., 2010;  
571 Cao et al., 2018). Thus, nighttime oxidation is not likely to lead to shorter VOC lifetimes  
572 than those calculated for daytime OH oxidation. In all, it is unlikely that the emissions of  
573 the target compounds in this study were substantially influenced by oxidative losses in  
574 the ambient atmosphere, and were predominantly driven by the magnitude of emissions  
575 in NYC and their atmospheric dilution. Yet, the observed ambient concentrations of  
576 different species could be potentially affected by the extent of their indoor vs. outdoor  
577 usage, seasonal patterns in applications (e.g., wintertime outdoor use of ethylene glycol  
578 as antifreeze), or physical processes related to their sources or sinks (e.g. partitioning).

579  
580

### 581 **3.3. Ambient measurements across diverse chemical classes**

582 Within the broader distribution of ion signals across the entire ambient mass spectra, we  
583 identified a diversity of chemical species. A selection of the most prominent ions in  
584 various compound categories are discussed in this section. Table [S4S7](#) summarizes  
585 different use sectors, but the vast majority have uses in personal care products,  
586 fragrances, a wide range of solvents, and/or other volatile consumer products. As such,  
587 some of the most abundant ions observed here were related to compounds found in the  
588 formulations of these types of products and/or had large annual production volumes (U.S.  
589 Environmental Protection Agency, Chemical Data Reporting, 2016). For some volatile  
590 compounds that exhibited low atmospheric abundances despite large annual production,  
591 it is possible that a substantial fraction of the production volume goes as feedstock to  
592 manufacture derivatives or are otherwise not prone to gas-phase emissions. Yet, seasonal  
593 differences in use, partitioning to the gas phase, and/or indoor-to-outdoor transport could  
594 also contribute to potential inter-annual variations.

595

596 The ions above 100 **parts per trillion** (ppt) on average included those with contributions  
 597 from acetates,  $C_2H_6O$  (e.g. ethylene glycol),  $C_3H_6O$  (e.g. acetone),  $C_2H_3N$  (e.g.  
 598 acetonitrile),  $C_{10}H_{16}$  (e.g. monoterpenes),  $C_4H_8O$  (e.g. methyl ethyl ketone) and  $C_5H_8O_2$   
 599 (e.g. methyl methacrylate) (Table 1). A detailed discussion of the trends in concentrations  
 600 and ion abundances of these and other ions is presented below and separated into distinct  
 601 categories based on chemical class or use-type.

602 **Table 1. List of ions calibrated with authentic standards (Table S2), probable  
 603 contributing isomers, geometric mean concentrations (with standard deviations),  
 604 annual emissions in each inventory, and mean concentration enhancement ratios  
 605 (with standard deviations of the mean and linear correlation coefficients) with  
 606 acetone and other prominent combustion-related tracers. Isomer identifications  
 607 marked with asterisks (\*) were confirmed in offline GC-EI-MS measurements, with  
 608 additional possible isomers included in Table S4S7.**

Compound formula, i	Probable compounds, i	Geo. mean concentration, ppt, i	Emissions, kg yr <sup>-1</sup> VCP <sup>†</sup> , FIVE- VCP	Ratios to tracer compounds ( $\Delta i/\Delta mol$ ) <sup>†</sup>			
				$\Delta i/\Delta Benzene$ (r)	$\Delta i^*1000/\Delta CO$ (r)	$\Delta i/\Delta Acetone$ (r)	$\Delta i/\Delta Benzyl alcohol$ (r)
$C_2H_6O_2$	Ethylene glycol	2437±3622	361511, <a href="#">260540236310</a> <a href="#">1333642</a>	1.1E+01±1.7E+00 (0.79)	9.1E+00±1.3E+00 (0.83)	2.8E+00±4.3E-01 (0.95)	3.0E+02±4.2E+01 (0.88)
$C_3H_6O$	Acetone*	977±783	<a href="#">16475481360720</a> , <a href="#">1587220</a>	3.8E+00±4.8E-01 (0.83)	3.3E+00±3.7E-01 (0.87)	--	1.1E+02±1.1E+01 (0.92)
$C_4H_8O_2$	Methyl acrylate*, Diacetyl*	810±396	1905, 4638	2.1E+00±2.5E-01 (0.82)	1.8E+00±1.9E-01 (0.89)	5.6E-01±6.1E-02 (0.95)	5.9E+01±5.6E+00 (0.94)
$C_4H_8O_2$	Ethyl acetate*, Butyric acid	679±664	<a href="#">27958</a> , <a href="#">32330225</a> , <a href="#">293</a>	2.8E+00±3.6E-01 (0.72)	2.3E+00±2.8E-01 (0.73)	7.2E-01±8.9E-02 (0.73)	7.6E+01±8.5E+00 (0.67)
$C_5H_8O_2$	Methyl acetate*, Propionic acid*, Hydroxyacetone, Ethyl formate	435±377	50747, <a href="#">114453103808</a>	1.7E+00±2.2E-01 (0.64)	1.5E+00±1.6E-01 (0.65)	4.5E-01±5.3E-02 (0.76)	4.8E+01±5.0E+00 (0.7)
$C_2H_3N$	Acetonitrile	246±102		8.5E-01±9.0E-02 (0.32)	7.2E-01±6.4E-02 (0.24)	2.2E-01±2.2E-02 (0.35)	2.3E+01±1.9E+00 (0.33)
$C_{10}H_{16}$	Monoterpenes (e.g., limonene*, $\alpha$ -Pinene*)	156±105	<a href="#">60206</a> , <a href="#">1710760327</a> , <a href="#">15516</a> <a href="#">44369</a>	5.1E-01±6.5E-02 (0.79)	4.3E-01±4.9E-02 (0.87)	1.3E-01±1.6E-02 (0.85)	1.4E+01±1.5E+00 (0.94)
$C_4H_8O$	MEK, THF, Cyclopropyl carbinol*	126±82	<a href="#">29375257457</a> , <a href="#">277556</a>	4.3E-01±5.1E-02 (0.79)	3.7E-01±3.8E-02 (0.84)	1.1E-01±1.2E-02 (0.93)	1.2E+01±1.1E+00 (0.85)
$C_3H_{10}O_2$	Isopropyl acetate*, n- propyl acetate*	114±106	<a href="#">2845</a> , <a href="#">58313457</a> , <a href="#">5289</a>	4.4E-01±5.7E-02 (0.61)	3.7E-01±4.4E-02 (0.69)	1.1E-01±1.4E-02 (0.69)	1.2E+01±1.3E+00 (0.58)
$C_5H_{10}O_2$	Methyl methacrylate*	108±121	1102, -	4.1E-01±6.0E-02 (0.45)	3.5E-01±4.7E-02 (0.37)	1.1E-01±1.5E-02 (0.5)	1.1E+01±1.5E+00 (0.41)
$C_6H_{12}O_2$	Butyl acetate*	103±138	<a href="#">74432</a> , <a href="#">6269280120</a> , <a href="#">56862</a>	4.9E-01±6.9E-02 (0.76)	4.1E-01±5.4E-02 (0.77)	1.3E-01±1.7E-02 (0.87)	1.3E+01±1.7E+00 (0.83)
$C_5H_{10}O_2$	Methyl benzoate*	92±15		1.1E-01±1.2E-02 (0.72)	9.1E-02±8.4E-03 (0.75)	2.8E-02±2.8E-03 (0.78)	3.0E+00±2.5E-01 (0.79)
$C_8H_{16}O_2$	Caprylic acid* (i.e., Octanoic acid), hexyl acetate	87±47	5281, -	2.5E-01±2.9E-02 (0.81)	2.1E-01±2.2E-02 (0.92)	6.5E-02±7.2E-03 (0.92)	6.9E+00±6.6E-01 (0.95)
$C_3H_8O_2$	2-Methoxy ethanol, propylene glyco*	82±51	240692, -	2.9E-01±3.3E-02 (0.71)	2.4E-01±2.4E-02 (0.71)	7.5E-02±8.0E-03 (0.85)	7.9E+00±7.3E-01 (0.77)
$C_9H_{18}O_2$	Methyl octanoate, Nonanoic acid*	77±24		1.4E-01±1.6E-02 (0.79)	1.2E-01±1.2E-02 (0.9)	3.7E-02±3.9E-03 (0.9)	3.9E+00±3.5E-01 (0.94)
$C_7H_6O$	Benzaldehyde*	76±37	<a href="#">142</a> , <a href="#">23156</a> , <a href="#">14833</a>	2.1E-01±2.5E-02 (0.83)	1.8E-01±1.8E-02 (0.88)	5.4E-02±6.1E-03 (0.88)	5.7E+00±5.6E-01 (0.93)
$C_{15}H_{24}$	Sesquiterpenes (e.g., $\beta$ - Caryophyllene)	70±11		7.3E-02±8.3E-03 (0.73)	6.2E-02±6.1E-03 (0.83)	1.9E-02±2.0E-03 (0.78)	2.0E+00±1.8E-01 (0.9)
$C_6H_{12}O$	2-Hexanone*, 4-Methyl- 2-pentanone	59±42	6162, <a href="#">1652714990</a>	2.0E-01±2.5E-02 (0.83)	1.7E-01±1.9E-02 (0.84)	5.3E-02±6.1E-03 (0.92)	5.6E+00±5.7E-01 (0.91)
$C_3H_6O_2$	Benzoic acid*	59±9		5.8E-02±6.3E-03 (0.48)	4.9E-02±4.6E-03 (0.39)	1.5E-02±1.5E-03 (0.4)	1.6E+00±1.4E-01 (0.45)
$C_4H_6O$	MVK, MACR	58±39		1.9E-01±2.4E-02 (0.83)	1.6E-01±1.8E-02 (0.87)	4.9E-02±5.9E-03 (0.94)	5.1E+00±5.5E-01 (0.94)
$C_8H_{14}O_2$	Cyclohexyl acetate	43±20		1.2E-01±1.4E-02 (0.81)	1.0E-01±1.0E-02 (0.89)	3.2E-02±3.4E-03 (0.95)	3.4E+00±3.0E-01 (0.95)
$C_9H_{10}O_2$	Benzyl acetate	39±19	7, -	1.0E-01±1.2E-02 (0.82)	8.8E-02±9.0E-03 (0.89)	2.7E-02±3.0E-03 (0.87)	2.9E+00±2.7E-01 (0.95)

<chem>C6H10O3</chem>	Dipropylene glycol	36±28	41085, <a href="#">#16574105732</a>	1.4E-01±1.7E-02 (0.65)	1.2E-01±1.3E-02 (0.71)	3.6E-02±4.1E-03 (0.7)	3.8E+00±3.8E-01 (0.8)
<chem>C4H10O3</chem>	Diethylene glycol	32±17	7026, <a href="#">#122345110939</a>	8.9E-02±1.1E-02 (0.84)	7.5E-02±7.9E-03 (0.87)	2.3E-02±2.6E-03 (0.91)	2.4E+00±2.4E-01 (0.92)
<chem>CH10H20O</chem>	Menthol, Decanal*	31±18	971, 0. <a href="#">#0605</a>	9.4E-02±1.1E-02 (0.77)	7.9E-02±8.2E-03 (0.89)	2.4E-02±2.7E-03 (0.9)	2.6E+00±2.5E-01 (0.96)
<chem>C3H8O</chem>	Cyclopentanone	30±16		8.4E-02±9.8E-03 (0.84)	7.1E-02±7.2E-03 (0.9)	2.2E-02±2.4E-03 (0.95)	2.3E+00±2.2E-01 (0.95)
<chem>C4H10O2</chem>	2-Butoxyethanol*, 1-propoxy-2-propanol*	23±19	<a href="#">#107758</a> , <a href="#">#79520109288, 72125</a>	8.9E-02±1.1E-02 (0.8)	7.5E-02±8.2E-03 (0.87)	2.3E-02±2.7E-03 (0.91)	2.4E+00±2.5E-01 (0.9)
<chem>C6H12O4Si4</chem>	D4 siloxane*	23±3	12872, <a href="#">#10221392707</a>	2.3E-02±2.5E-03 (0.38)	2.0E-02±1.8E-03 (0.48)	6.0E-03±6.1E-04 (0.48)	6.4E-01±5.5E-02 (0.59)
<chem>C4H30O4</chem>	TXIB*	18±4	- , <a href="#">#24962264</a>	2.6E-02±3.0E-03 (0.73)	2.2E-02±2.2E-03 (0.83)	6.8E-03±7.2E-04 (0.75)	7.2E-01±6.5E-02 (0.86)
<chem>C10H12O2</chem>	Eugenol	16±5	45, -	3.1E-02±3.5E-03 (0.82)	2.6E-02±2.5E-03 (0.85)	7.9E-03±8.4E-04 (0.91)	8.4E-01±7.6E-02 (0.92)
<chem>C4H20O3</chem>	Dipropylene glycol propyl ether	16±4	4150, <a href="#">#65785966</a>	2.3E-02±2.7E-03 (0.65)	2.0E-02±2.0E-03 (0.71)	6.1E-03±6.5E-04 (0.62)	6.4E-01±5.9E-02 (0.73)
<chem>C12H16O3</chem>	2-Phenoxyethyl isobutyrate	16±2		1.6E-02±1.7E-03 (0.73)	1.3E-02±1.2E-03 (0.76)	4.1E-03±4.1E-04 (0.79)	4.4E-01±3.6E-02 (0.83)
<chem>C11H30O5Si5</chem>	D5 siloxane*	16±15	<a href="#">#272778</a> , <a href="#">#357202323982</a>	6.7E-02±8.5E-03 (0.7)	5.7E-02±6.4E-03 (0.82)	1.7E-02±2.1E-03 (0.82)	1.8E+00±2.0E-01 (0.9)
<chem>C12H14O4</chem>	Diethyl phthalate*	15±3	17138, -	2.3E-02±2.4E-03 (0.64)	1.9E-02±1.7E-03 (0.7)	5.9E-03±5.8E-04 (0.65)	6.2E-01±5.1E-02 (0.71)
<chem>C7H8O</chem>	Benzyl alcohol	14±6	22898, <a href="#">#2292320791</a>	3.6E-02±4.1E-03 (0.85)	3.1E-02±3.0E-03 (0.92)	9.5E-03±1.0E-03 (0.92)	--
<chem>C8H10O</chem>	6-Methyl 5-hepten-2-one	14±7		4.1E-02±4.6E-03 (0.81)	3.4E-02±3.4E-03 (0.89)	1.1E-02±1.1E-03 (0.96)	1.1E+00±1.0E-01 (0.96)
<chem>C5H8O3</chem>	Methyl paraben	14±4		2.4E-02±2.7E-03 (0.83)	2.1E-02±2.0E-03 (0.86)	6.3E-03±6.6E-04 (0.83)	6.7E-01±6.0E-02 (0.87)
<chem>C4H10O2</chem>	1-Methoxy-2-propanol*	13±8	<a href="#">#3405, 24053558,</a> <a href="#">#2182</a>	4.1E-02±4.9E-03 (0.78)	3.5E-02±3.6E-03 (0.85)	1.1E-02±1.2E-03 (0.89)	1.1E+00±1.1E-01 (0.89)
<chem>C5H8O2</chem>	Furfural*	13±6	- , 0.01	3.4E-02±4.0E-03 (0.71)	2.9E-02±2.9E-03 (0.62)	8.8E-03±9.7E-04 (0.56)	9.3E-01±8.9E-02 (0.66)
<chem>C4H10O</chem>	Cyclohexanone	12±6	384, <a href="#">#10665396838</a>	3.6E-02±4.1E-03 (0.84)	3.0E-02±3.0E-03 (0.91)	9.4E-03±1.0E-03 (0.96)	9.9E-01±9.1E-02 (0.92)
<chem>C4H12O3</chem>	PGMEA*, 2-Ethoxyethyl acetate	12±11	<a href="#">#40017, 824410327,</a> <a href="#">#7450</a>	4.7E-02±6.0E-03 (0.78)	4.0E-02±4.6E-03 (0.76)	1.2E-02±1.5E-03 (0.9)	1.3E+00±1.4E-01 (0.86)
<chem>C6H8O3</chem>	Maltol	11±3		1.3E-02±1.6E-03 (0.59)	1.1E-02±1.2E-03 (0.44)	3.4E-03±3.8E-04 (0.42)	3.6E-01±3.5E-02 (0.49)
<chem>C8H8O</chem>	Acetophenone*	10±6	4, -	3.2E-02±3.8E-03 (0.81)	2.7E-02±2.9E-03 (0.85)	8.4E-03±9.4E-04 (0.89)	8.8E-01±8.7E-02 (0.9)
<chem>C4H8NO</chem>	Methyl pyrrolidone	9±3	12749, <a href="#">#1545214015</a>	1.9E-02±2.2E-03 (0.72)	1.6E-02±1.6E-03 (0.78)	5.0E-03±5.3E-04 (0.77)	5.3E-01±4.8E-02 (0.78)
<chem>C4H10O2</chem>	Phenoxyethanol*	9±3	9851, <a href="#">#02523</a>	1.7E-02±2.0E-03 (0.78)	1.5E-02±1.5E-03 (0.84)	4.5E-03±4.9E-04 (0.86)	4.8E-01±4.4E-02 (0.91)
<chem>C8H18O3</chem>	2-(2-Butoxyethoxy)ethanol, DGBE	8±4	<a href="#">#48389, 6827048681,</a> <a href="#">#62011</a>	2.1E-02±2.4E-03 (0.85)	1.8E-02±1.8E-03 (0.91)	5.4E-03±5.9E-04 (0.89)	5.7E-01±5.4E-02 (0.94)
<chem>C10H10O4</chem>	Dimethyl phthalate	7±1	70, -	9.1E-03±1.0E-03 (0.62)	7.7E-03±7.4E-04 (0.62)	2.4E-03±2.5E-04 (0.55)	2.5E-01±2.2E-02 (0.65)
<chem>C12H20O3</chem>	Texanol*	7±4	<a href="#">#497658179276</a>	2.0E-02±2.4E-03 (0.57)	1.7E-02±1.8E-03 (0.74)	5.3E-03±5.9E-04 (0.67)	5.6E-01±5.5E-02 (0.74)
<chem>C9H10O3</chem>	Ethyl paraben	6±1		7.0E-02±7.7E-04 (0.84)	5.9E-03±5.6E-04 (0.84)	1.8E-03±1.9E-04 (0.85)	1.9E-01±7.7E-02 (0.9)
<chem>C11H14O3</chem>	Butyl paraben	6±1		8.5E-03±9.0E-04 (0.71)	7.2E-03±6.5E-04 (0.74)	2.2E-03±2.2E-04 (0.8)	2.3E-01±9.6E-02 (0.76)
<chem>C6H10O3</chem>	Ethyl acetoacetate	4±2		1.3E-02±1.5E-03 (0.85)	1.1E-02±1.1E-03 (0.87)	3.4E-03±3.7E-04 (0.93)	3.6E-01±3.4E-02 (0.91)
<chem>C10H12O</chem>	Benzyl acetone	4±2		1.0E-02±1.2E-03 (0.85)	8.5E-03±8.8E-04 (0.91)	2.6E-03±2.9E-04 (0.94)	2.8E-01±2.6E-02 (0.97)
<chem>C7H12O4</chem>	Pentadioic acid, dimethyl ester	4±1	4942, <a href="#">#2823225606</a>	7.2E-03±8.0E-04 (0.8)	6.1E-03±5.8E-04 (0.84)	1.9E-03±1.9E-04 (0.87)	2.0E-01±1.7E-02 (0.89)
<chem>C10H12O3</chem>	Propyl paraben	4±1		6.3E-03±7.1E-04 (0.54)	5.3E-03±5.3E-04 (0.46)	1.6E-03±1.7E-04 (0.42)	1.7E-01±1.6E-02 (0.51)
<chem>C10H20O2</chem>	Hydroxycitronellal	3±1		5.3E-03±5.9E-04 (0.78)	4.5E-03±4.3E-04 (0.88)	1.4E-03±1.4E-04 (0.92)	1.5E-01±1.3E-02 (0.95)
<chem>C8H18O2</chem>	Ethylene glycol hexyl ether*, 1,2-Octandiol	2±1	15836, <a href="#">#85447749</a>	5.8E-03±6.7E-04 (0.8)	4.9E-03±4.9E-04 (0.88)	1.5E-03±1.6E-04 (0.87)	1.6E-01±1.5E-02 (0.94)
<chem>C3H8O3</chem>	Glycerol	1±0.5	148441, <a href="#">#1046753949405</a>	3.0E-03±3.5E-03- <a href="#">#04±1.8E-04 (0.6664)</a>	2.1E-03±2.4E-04 (0.47)	5.5E-04±5.8E-05 (0.45)	86.3E-02±7.6E8E-03 (0.7473)
<chem>C4H10O4</chem>	Triethyleneglycol	1±0.3	1718, <a href="#">#1052955</a>	2.1E-03±2.4E-04 (0.47)	1.8E-03±1.7E-04 (0.45)	5.5E-04±5.8E-05 (0.4)	5.8E-02±5.2E-03 (0.51)

609 <sup>†</sup> **Note****Note**: For comparison to the emissions inventories, the standard deviation of the mean was used for the compound ratios to constrain the uncertainty of the average compound ratios over the 10-day period, yet we note that higher time resolution variations in the observed ratios are expected given the spatiotemporal variations in emissions from contributing sources distributed around the site.

611 The listed mean concentrations are calculated from hourly averages of data sampled at 1 Hz throughout the measurement period.

612 Given the varied correlation coefficients against tracers (Figure 6), to reduce bias, background-subtracted geometric means are used to

613 **Formatted: Font: Bold**

614 determine the compound ratios, though the geometric mean ratios and slopes are similar, especially for well-correlated compound  
615 pairs (Figure S14S13). In the case of glycerol, given its low ambient concentration, the observed background level (i.e. 5th percentile)  
616 was 0.1 ppt below its calculated limit of detection. Based on this, the glycerol ratio to acetone for the purposes of Figure 7's  
617 comparison was determined based on their regression (5.3 E-04 mol/mol;  $r=0.74$ ) when removing <LOD values. This has minimal  
618 influence on the glycerol-related conclusions related to its substantially low relative abundance as the geometric mean enhancement  
619 ratio calculation yielded a similar result (7.9E-04 mol/mol) when including all observations (Figure S13).

620

### 621 3.3.1 Esters

622 Prominent esters observed in this study and discussed here include acetates and acrylates.  
623  $C_3H_6O_2$ ,  $C_4H_6O_2$ ,  $C_4H_8O_2$ ,  $C_5H_{10}O_2$  and  $C_6H_{12}O_2$  were ions with some of the highest  
624 ambient concentrations in our data whose geometric mean concentrations varied between  
625 0.1-0.8 ppb (Figure 4a-f). Small acetates (e.g. methyl-, ethyl-, propyl- and butyl- acetates)  
626 are likely major contributors to these ion signals since they are being extensively used as  
627 oxygenated solvents and contribute to natural and designed fragrances/flavorings. The  
628 VCPy $\pm$  model estimates the annual emissions of these acetates to be on the order of  $10^4$ -  
629  $10^5$  kg  $yr^{-1}$  in NYC, but other compounds can also contribute to these ions. For example,  
630 hydroxyacetone and propionic acid may add to  $C_3H_6O_2$ , diacetyl and  $\gamma$ -butyrolactone to  
631  $C_4H_6O_2$ , methyl propionate and butyric acid to  $C_4H_8O_2$ , isobutyl formate to  $C_5H_{10}O_2$ , and,  
632 diacetone alcohol and methyl pentanoate to  $C_6H_{12}O_2$ . However, their estimated emissions  
633 are 1-2 orders of magnitude smaller than each of the acetates, likely making them minor  
634 contributors to observed ion intensities.  $C_8H_{14}O_2$  (e.g. cyclohexyl acetate) and  $C_9H_{10}O_2$   
635 (e.g. benzyl acetate) were also important ions within this category with average  
636 concentrations at  $40 \pm 20$  ppt and peaks reaching up to 150 ppt during the measurement  
637 period.

638

639 We observed hourly  $C_5H_8O_2$  concentrations exceeding 1 ppb (Figure 5), which includes  
640 methyl methacrylate (MMA) and potential contributions from 2,3-pentanedione and ethyl  
641 acrylate given their use as solvents in various coatings and inks. MMA sees some use in  
642 adhesives, paints and safety glazing (estimated emissions  $\sim 10^3$  kg  $yr^{-1}$ ; VCPy $\pm$ ), but  
643 could also potentially be emitted from the common polymer poly-(methyl methacrylate)  
644 (PMMA) which is used in plastic materials. With a geometric mean concentration of  $100$   
645  $\pm 120$  ppt, possible contributions of PMMA offgassing/degradation as a source of  
646 ambient MMA warrants further investigation, but has been observed in polymer studies  
647 (Bennet et al., 2010). In addition to isomer-specific observations of MMA, we note that  
648 most of the acetates were also confirmed via offline measurements using adsorbent tubes  
649 that were analyzed using GC EI-MS for compound-specific identification (Table 1).

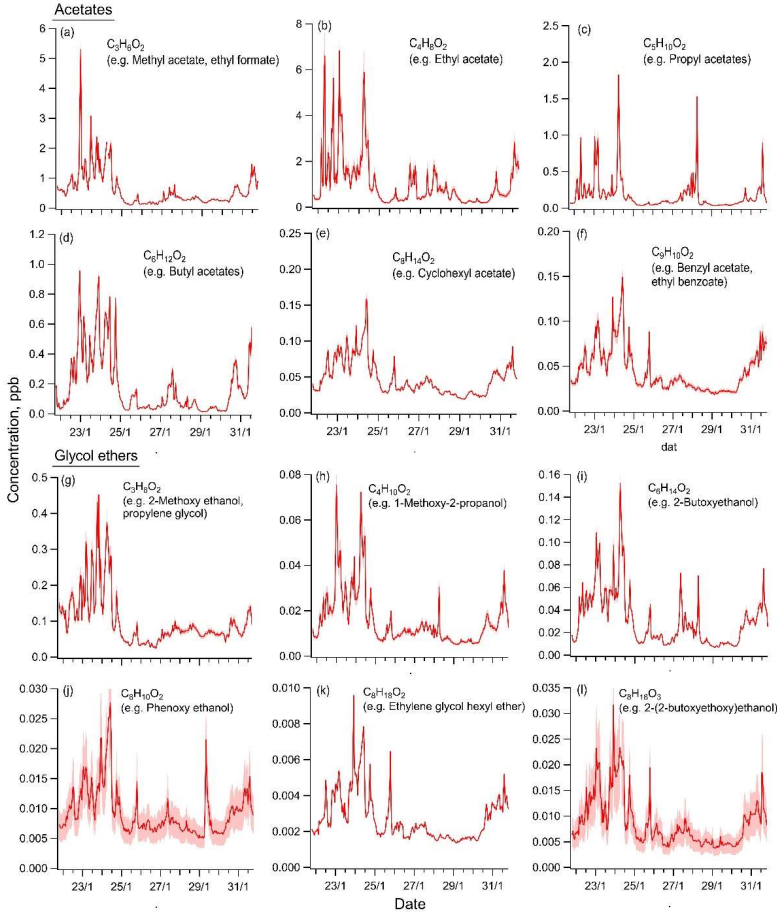
650

651

### 652 3.3.2 Carbonyls

653

654 Carbonyls are also extensively used as replacements for non-polar solvents in various  
 655 consumer/commercial applications along with use in cosmetics and personal care  
 656 products. Hence,  $C_3H_6O$  (e.g. acetone),  $C_4H_8O$  (e.g. methyl ethyl ketone) and  $C_6H_{12}O$   
 657 (e.g. methyl butyl ketone) were expectedly present at relatively high concentrations.  
 658 Given the absence of considerable known emissions of other isomers, the ion intensities  
 659 were mainly attributed to these carbonyl compounds.

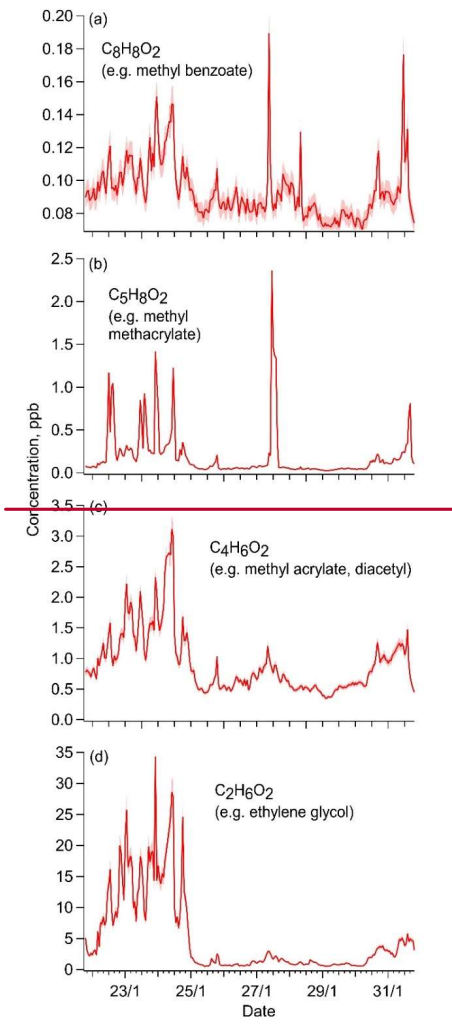


660

661 **Figure 4. The concentration timeseries of select, widely-used acetates and glycol**  
 662 **ethers. Timeseries are shown with major isomers as examples with a more**

663 comprehensive list available in Tables 1 and [S4S7](#). Displayed uncertainty bands are  
664 a function of calibration uncertainties (including for isomer pairs) ([Table S2](#)).  
665

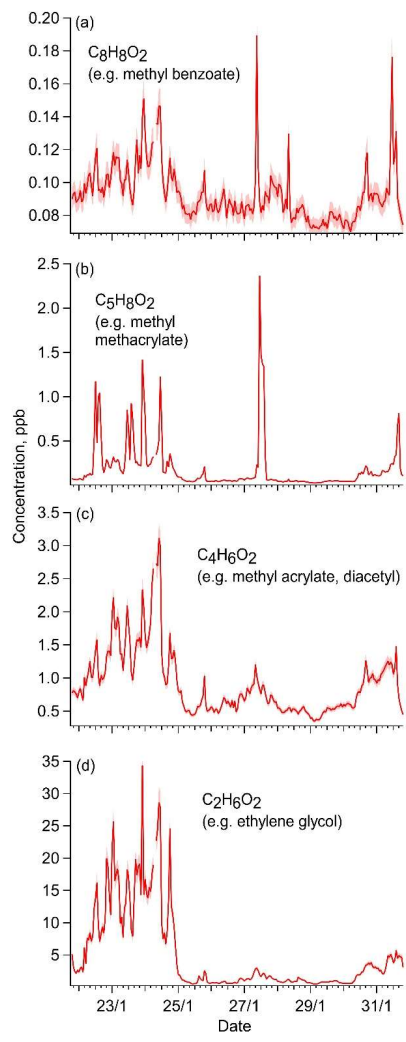
666 Given the absence of considerable known emissions of isomers, the ion intensities were  
667 mainly attributed to these carbonyl compounds. Acetone showed the highest average  
668 concentrations in urban air among all carbonyl solvents detected (Table 1). Since  
669 biogenic and secondary sources of acetone (i.e. from atmospheric oxidation) are  
670 relatively limited in NYC wintertime conditions, the measurements are consistent with  
671 very high anthropogenic emissions in NYC ( $\sim 10^6 \text{ kg yr}^{-1}$ ) and extensive use in products  
672 and by industries ( $\sim 10^9 \text{ kg yr}^{-1}$  nationwide).



673

674 We acknowledge that other primary and secondary sources may also exist for some  
 675 carbonyl species, including unknown contributions from combustion-related sources,  
 676 cooking or other anthropogenically-influenced sources. Yet, VCPs are the dominant  
 677 source of acetone in NYC as per the latest emissions inventories (VCPy+ and FIVE-  
 678 VCP) and recent source apportionment of wintertime mobile measurements in NYC that  
 679 attribute most of the observed acetone signal to the VCP-related source factor (Gkatzelis  
 680 et al., 2021b).

681 Acetone showed the highest average concentrations in urban air among all carbonyl  
682 solvents detected (Table 1). Since biogenic and local secondary sources of acetone (i.e.  
683 from atmospheric oxidation) are relatively reduced in NYC wintertime conditions, the  
684 measurements are consistent with very high anthropogenic emissions in NYC (~10<sup>6</sup> kg  
685 yr<sup>-1</sup>) and extensive use in products and by industries (~10<sup>9</sup> kg yr<sup>-1</sup> nationwide), and  
686 recent work on acetone in NYC (Gkatzelis et al., 2021b).



687

688 **Figure 5. Concentration timeseries of select prominent ions that include**  
689 **contributions from major VCP-related compounds (examples listed; see Tables 1**  
690 **and [S4S7](#) for expanded list).**

691

692 MEK was the second highest carbonyl observed with C<sub>4</sub>H<sub>8</sub>O ion concentration spanning  
693 from 50 to over 500 ppt. Its estimated emissions are 0.4-3 x10<sup>5</sup> kg yr<sup>-1</sup> or greater in NYC  
694 and it finds significant use in coatings with large annual nationwide consumption (~10<sup>8</sup>  
695 kg yr<sup>-1</sup>). Methyl butyl ketone (MBK) and cyclohexanone were the next most abundant in  
696 this category. The average concentration of MBK at 58 ± 42 ppt was nearly 50% of MEK  
697 but reached up to 300 ppt during the initial 4 days of the sampling period. Cyclohexanone  
698 however was much smaller at 12 ± 7 ppt with highest concentrations reaching up to only  
699 35 ppt across the measurement period, which was consistent with its emissions in VCPy<sub>±</sub>  
700 (~400 kg yr<sup>-1</sup>) being at least two orders of magnitude smaller than other species in this  
701 category, though its estimated emissions in FIVE-VCP were much higher (Table 1).

702

703

### 704 **3.3.3 Glycols and glycol ethers**

705 Glycols and glycol ethers are compound classes that have been traditionally challenging  
706 to measure in real-time with PTR-ToF instruments, being prone to ionization-induced  
707 fragmentation during online sampling. With Vocus CI-ToF, we were able to measure  
708 signals of several glycol and glycol ether compounds. The most prominent ones included  
709 C<sub>2</sub>H<sub>6</sub>OC<sub>2</sub>H<sub>6</sub>O<sub>2</sub>, C<sub>3</sub>H<sub>8</sub>O<sub>2</sub>, C<sub>6</sub>H<sub>14</sub>O<sub>2</sub> and C<sub>4</sub>H<sub>10</sub>O<sub>2</sub> ions whose concentrations ranged  
710 between 10-500 ppt across the sampling period (Figure 4g-l) with C<sub>2</sub>H<sub>6</sub>OC<sub>2</sub>H<sub>6</sub>O<sub>2</sub>  
711 reaching ppb-levels.

712

713 C<sub>2</sub>H<sub>6</sub>O<sub>2</sub> (e.g. ethylene glycol) was the most abundant observed compound in this study  
714 (Table 1). The emissions of ethylene glycol in NYC are estimated to be on the order of 3-  
715 4x10<sup>5</sup> kg yr<sup>-1</sup> which is a factor of 3 smaller than acetone (~10<sup>6</sup> kg yr<sup>-1</sup>; VCPy<sub>±</sub> and FIVE-  
716 VCP). Still the mean concentration of C<sub>2</sub>H<sub>6</sub>O<sub>2</sub> (2.4 ± 3.6 ppb) was found to be  
717 considerably larger than that of C<sub>3</sub>H<sub>6</sub>O (0.95 ± 0.73 ppb). This difference in their relative  
718 ratio could not be explained by their atmospheric lifetimes since ethylene glycol is  
719 estimated to be considerably shorter lived than acetone (1.5 vs 33 days).

720

721 The C<sub>3</sub>H<sub>8</sub>O<sub>2</sub> ion (20-450 ppt) likely represented propylene glycol, which was the highest  
722 emitted isomer in NYC (~10<sup>5</sup> kg yr<sup>-1</sup>; VCPy<sub>±</sub> and FIVE-VCP) estimates with  
723 comparatively minor contributions from 2-methoxy ethanol and dimethoxymethane, all  
724 of which are used as solvents in varnishes and various cosmetics. C<sub>6</sub>H<sub>14</sub>O<sub>2</sub>, including 2-

725 butoxyethanol, a coupling agent in water-based coatings as well as solvent in varnishes,  
726 inks, cleaning products and resins, was observed at 10-150 ppt. The estimated emissions  
727 of isomer hexylene glycol are 100 times smaller and would likely not have contributed  
728 much to the C<sub>6</sub>H<sub>14</sub>O<sub>2</sub> ion signal.

729

730 C<sub>4</sub>H<sub>10</sub>O<sub>2</sub>, which ranged 10-80 ppt, includes 1-methoxy-2-propanol and 2-ethoxyethanol  
731 as both are used as organic solvents in industrial and commercial applications. Based on  
732 emissions estimates, 1-methoxy-2-propanol is expected to be the dominant contributor to  
733 this signal with NYC emissions of  $\sim 2\text{-}3 \times 10^3 \text{ kg yr}^{-1}$ , which are 30-50 times higher than 2-  
734 ethoxyethanol in estimates. C<sub>6</sub>H<sub>12</sub>O<sub>3</sub> varied over a similar concentration range (5-80 ppt)  
735 resulting from propylene glycol methyl ether acetate (a.k.a. PGMEA) emissions ( $\sim 0.7\text{-}$   
736  $1 \times 10^4 \text{ kg yr}^{-1}$ ). The estimated emissions of the other likely isomer, 2-ethoxyethyl acetate,  
737 were lower by a factor of 100. Relatively smaller concentrations of C<sub>8</sub>H<sub>10</sub>O<sub>2</sub>, C<sub>8</sub>H<sub>18</sub>O<sub>2</sub>  
738 and C<sub>8</sub>H<sub>18</sub>O<sub>3</sub> ranging between 2-30 ppt were also observed (Figure 4j-l) which include  
739 glycol ethers based on their higher emissions relative to other isomers.

740

741

### 742 3.3.4 Select compounds related to personal care products

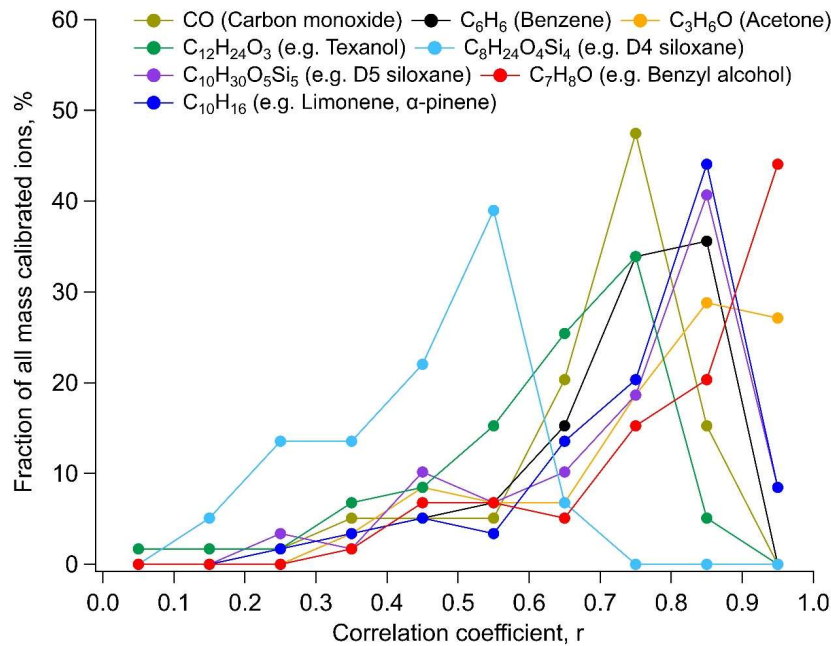
743

744 Many personal care products routinely include D5 which is often used as a tracer for  
745 emissions from this source category (Gkatzelis et al., 2021a). Hence, we attributed all of  
746 the measured C<sub>10</sub>H<sub>30</sub>O<sub>5</sub>Si<sub>5</sub> ion abundance to D5 in this study. Both the VCPy<sup>+</sup> and FIVE-  
747 VCP inventories estimate the annual emissions of D5 to be slightly higher ( $\sim 10^5 \text{ kg yr}^{-1}$ )  
748 than common oxygenated solvents, e.g. esters. However, its ambient concentration was  
749 found to be much lower in comparison to them and other oxygenated solvents, varying  
750 from 10 ppt to 140 ppt during the 10-day period with a geometric mean of 16 ppt. Other  
751 studies report similar concentrations in U.S. cities (Coggon et al., 2018; Stockwell et al.,  
752 2021). ~~Compared to the emissions inventories, ambient concentrations were lower by a~~  
753 ~~factor of 2, potentially due to wintertime conditions (e.g. partitioning), the relative~~  
754 ~~amount emitted indoors vs outdoors, and/or limitations in indoor to outdoor~~  
755 ~~transport. Compared to the emissions inventories, the expected ambient concentrations~~  
756 ~~relative to acetone were lower by a factor of 2 (see Section 3.5, Table 1). Hypotheses for~~  
757 ~~this difference include potential variations with wintertime conditions (e.g. partitioning),~~  
758 ~~the relative amount emitted indoors vs outdoors, limitations in indoor-to-outdoor~~  
759 ~~transport with reduced wintertime ventilation and/or D5's behavior as a semi-volatile~~  
760 ~~species in the presence of indoor condensational reservoirs (Abbatt and Wang, 2020;~~  
761 ~~Wang et al., 2020).~~ The distinct enhancement in ambient concentrations of D5 in the  
762 morning and evening hours in incoming winds over Manhattan indicated that people were  
763 a dominant emissions pathway of D5 emissions in NYC. ~~Since most people spend~~

764 majority of their day indoors, D5 emissions are subjected to large with relatively less  
765 indoor sinks thereby dampening their contribution to outdoors and will likely-to-outdoor  
766 transport during the day, though that could be sensitive to reduced influenced wintertime  
767 ventilation conditions (Sheu et al., 2021; Wang et al., 2020). By comparison, while  
768 estimated emissions of benzyl alcohol in NYC were only ~20% of D5, it had similar  
769 average concentrations as D5 (Table 1) ranging from 8 to 40 ppt. With strong correlations  
770 with many VCP-related compounds (Figure 6), wide use in various consumer product  
771 formulations and a similar kOH to m-xylene (i.e.,  $\sim 10^{-11}$  molecule $^{-1}$  cm $^3$  s $^{-1}$ ), this  
772 suggestsbenzyl alcohol showed its potential as an additional VCP-related compound for  
773 routine monitoring/analysis.

774

775 The glycerol-related C<sub>3</sub>H<sub>8</sub>O<sub>3</sub> ion was especially interesting. Only 1-7 ppt was detected  
776 across the measurement period even though it is widely used in the personal care industry  
777 with estimated annual emissions in NYC on the order of 10<sup>5</sup> kg yr<sup>-1</sup>. However, Li et al  
778 show in a laboratory evaporation study that glycerol evaporation is much slower than  
779 expected (Li et al., 2018). Still, glycerol is expected to influence air quality based on its  
780 projected emissions (Gkatzelis et al., 2021b) and no other isomers exist with significant  
781 known emissions. Yet, the ratio of background-subtracted concentrations of C<sub>3</sub>H<sub>8</sub>O<sub>3</sub> to  
782 D5 ( $\Delta$ C<sub>3</sub>H<sub>8</sub>O<sub>3</sub>/ $\Delta$ D5) was 0.042035 despite a much higher ratio of estimated emissions (2,  
783 12 mol/mol: VCPy, $\pm$ , FIVE-VCP). This suggests that C<sub>3</sub>H<sub>8</sub>O<sub>3</sub> is significantly lower than  
784 would be expected based on D5-related activities, and, potentially points to limitations in  
785 evaporation, indoor-to-outdoor transport, or atmospheric partitioning—all of which could  
786 be influenced by wintertime conditions.



787

788 **Figure 6. A comparison of correlations to major tracer compounds. Distributions of**  
 789 **correlation coefficients (using hourly-average data) for Table 1 compounds against**  
 790 **select prominent compounds used as markers of VCP-related sources or general**  
 791 **anthropogenic emissions (e.g. CO, benzene). Results binned into 0.1 intervals; for**  
 792 **example, ~45% of compounds were highly-correlated at  $0.9 < r < 1$  with  $C_7H_8O$  (i.e.**  
 793 **benzyl alcohol). See SI for similar analysis including all uncalibrated target ions and**  
 794 **correlation comparisons for all target compounds (Figures S12-15, S17-S14-17, S19).**

795

796  $C_8H_8O_3$ ,  $C_9H_{10}O_3$ ,  $C_{10}H_{12}O_3$  and  $C_{11}H_{14}O_3$  are paraben-related ions, but additional  
 797 isomers (e.g. p-ethoxybenzoic acid for  $C_{11}H_{14}O_3$ ) might also contribute to these ion  
 798 signals. Several others are less likely to be found in the atmosphere since they are not  
 799 directly used in formulations of volatile chemical products but rather as feedstocks for  
 800 derivatives used in different industries. Some isomers such as vanillin and vanillylacetone  
 801 are also used in food flavoring. Methyl paraben-related  $C_8H_8O_3$  showed the highest  
 802 concentration among these four ions ranging from 8 to 35 ppt across the sampling period.  
 803 The remaining three had concentrations under 10 ppt throughout the sampling duration.

804

805 **3.3.5 Select IVOCs related to coatings**

806  
807 The  $C_{12}H_{24}O_3$  and  $C_{16}H_{30}O_4$  ions were primarily attributed to texanol and 2,2,4-trimethyl-  
808 1,3-pentanediol diisobutyrate (TXIB) emissions that are widely used in coatings  
809 (Gkatzelis et al., 2021a). Even though estimated emissions of texanol ( $1.9\text{--}2.5 \times 10^5$  kg  
810  $yr^{-1}$ ) are much higher than TXIB (2500 kg  $yr^{-1}$ ; FIVE-VCP), and, texanol production on a  
811 national scale (45-110 Gg) considerably exceeds TXIB (22-44 Gg) (U.S. Environmental  
812 Protection Agency, Chemical Data Reporting, 2016), the concentrations of both these  
813 species had a similar range (5-30 ppt) with enhancements in TXIB concentrations above  
814 the 5<sup>th</sup> percentile background being comparable to texanol on average (Table 1). Given  
815 reduced photochemistry, this may suggest differences in outdoor vs indoor application,  
816 some geographical variability in their use and/or larger diversity in TXIB sources than  
817 texanol in this particular urban area.

818

819 **3.3.6 Phthalates and Fatty-acid methyl esters (FAMEs)**

820 Phthalates have received considerable attention in indoor environments but their  
821 concentrations in ambient air are relatively less constrained. In this study, the ion  
822 intensities of  $C_{10}H_{10}O_4$  and  $C_{12}H_{14}O_4$  include dimethyl phthalate (DMP) and diethyl  
823 phthalate (DEP), respectively, two commonly used phthalates in various consumer  
824 products.  $C_{10}H_{10}O_4$  and  $C_{12}H_{14}O_4$  had similar ion abundances across the 10-day sampling  
825 period. After accounting for differences in instrument response,  $C_{10}H_{10}O_4$  concentrations  
826 were found to be smaller than  $C_{12}H_{14}O_4$  throughout the campaign which aligns with DEP  
827 emission estimates being greater than DMP in NYC. The ambient concentrations of the  
828 two ions ranged between 5-30 ppt and often synchronously peaked between midnight and  
829 early morning hours (12-6 AM) while the lowest daily concentrations were observed  
830 during afternoons. These concentration trends indicated that unlike compounds associated  
831 with personal care products, phthalate concentrations were less influenced by outdoor  
832 human activities.

833

834 FAMEs are also an important class of compounds used in various consumer products. We  
835 identified  $C_9H_{18}O_2$  (e.g. methyl octanoate) and  $C_{11}H_{22}O_2$  (e.g. methyl decanoate) ions via  
836 CI-ToF that varied similarly in their abundances across the campaign period.  $C_9H_{18}O_2$   
837 concentrations ranged from 50 ppt to 200 ppt and showed slightly higher ion abundances  
838 than  $C_{11}H_{22}O_2$  even though the annual production of methyl octanoate for use in  
839 consumer/commercial products (0.5-9 Gg) is considerably lower than methyl decanoate  
840 (4.5-22 Gg) (U.S. Environmental Protection Agency, Chemical Data Reporting, 2016).  
841 This suggested that isomers such as heptyl acetate and propyl hexanoate, which are used  
842 in perfumes and food flavoring, may have also contributed to  $C_9H_{18}O_2$  signal. Emissions

843 of pentyl butyrate, which has uses such as an additive in cigarettes are also possible. The  
844 highest abundances in both C<sub>9</sub>H<sub>18</sub>O<sub>2</sub> and C<sub>11</sub>H<sub>22</sub>O<sub>2</sub> corresponded to wind currents from  
845 Manhattan as well as the Bronx, which infers comparable emission rates within New  
846 York City.

847

#### 848 **3.4 Other observed ions of interest**

849 Of the total ions measured, a subset of isomers covering diverse chemical functionalities  
850 were included for calibration while others were not calibrated or presented challenges  
851 associated with their physiochemical properties that caused transmission issues during  
852 LCS calibration. Hence, we will discuss trends in such ions in this subsection in terms of  
853 their measured ion abundances (Table S3, figure S9S11). These include ions with likely  
854 contributions from ethanolamines, organic acids, large alkyl methyl esters and some  
855 oxygenated terpenoid compounds that are used in a wide range of volatile chemical  
856 products.

857

858 Anthropogenic sources are major contributors of oxygenated terpenoid compounds (i.e.  
859 oxy-terpenoids) in many urban areas, especially during wintertime. Among relevant ions  
860 observed, C<sub>10</sub>H<sub>16</sub>O (e.g. camphor), C<sub>10</sub>H<sub>18</sub>O (e.g. linalool), C<sub>10</sub>H<sub>20</sub>O (calibrated with  
861 menthol) and C<sub>7</sub>H<sub>10</sub>O (e.g. norcamphor) were the most prevalent in terms of measured  
862 abundances. A number of isomers that are similarly used in various consumer products  
863 likely contributed to their signal intensities. It is interesting to note that C<sub>10</sub>H<sub>16</sub>O  
864 exhibited higher ion abundance than C<sub>10</sub>H<sub>18</sub>O despite comparable estimated emissions of  
865 camphor and linalool ( $\sim 10^3$  kg yr<sup>-1</sup>; VCPy~~+~~) in NYC. This could be due to differences in  
866 CI-ToF response factors, the magnitude of relative isomer contributions, seasonal trends  
867 in the use of chemical species, or uncertainties in fragrance speciation within emissions  
868 inventories. The peaks in abundances of all oxy-terpenoids were observed synchronously  
869 in the morning hours between 8-10 AM and in the evening between 6-8 PM, consistent  
870 with major commuting periods, especially when wind currents blew in from over  
871 Manhattan from the south and south-east where the outdoor activity peaks during  
872 morning and evening commute hours.

873

874 We detected C<sub>2</sub>H<sub>7</sub>NO, C<sub>4</sub>H<sub>11</sub>NO<sub>2</sub> and C<sub>6</sub>H<sub>15</sub>NO<sub>3</sub> ions at the site, representing  
875 ethanolamine, diethanolamine, and triethanolamine, respectively. Of these, C<sub>4</sub>H<sub>11</sub>NO<sub>2</sub>  
876 and C<sub>6</sub>H<sub>15</sub>NO<sub>3</sub> followed trends of other ~~VCPs~~<sup>VCP</sup>-related compounds. C<sub>4</sub>H<sub>11</sub>NO<sub>2</sub> showed  
877 the highest ion abundance throughout the campaign with the exception of a 24-hour  
878 period between 26/1 and 27/1 when C<sub>2</sub>H<sub>7</sub>NO abundances increased dramatically. This  
879 peak in C<sub>2</sub>H<sub>7</sub>NO was potentially caused by biomass burning since ions pertinent to 2-

880 methylfuran, methyl isocyanate, nitromethane and 2,5 dimethylfuran also peaked  
881 simultaneously during this period. The influence of biomass burning in all cases was  
882 subsequently filtered from the ion abundance timeseries prior to investigating their linear  
883 regressions with other species (figure S15). C<sub>4</sub>H<sub>11</sub>NO<sub>2</sub> showed much greater variations  
884 with wind patterns, more similar to other VCPs, and peaks were noted in early morning  
885 hours between 6-9 AM and during early evening hours around 6 PM. C<sub>6</sub>H<sub>15</sub>NO<sub>3</sub> showed  
886 lower signal relative to C<sub>2</sub>H<sub>7</sub>NO and C<sub>4</sub>H<sub>11</sub>NO<sub>2</sub> which could be attributed to its smaller  
887 annual production for use in consumer/commercial products (45-113 Gg), variations in  
888 CI-ToF response factors and/or lower volatility that could decrease emission timescales  
889 and cause it to partition to available surfaces indoors.

890

891 Several other major ions included C<sub>7</sub>H<sub>14</sub>O<sub>2</sub>, C<sub>8</sub>H<sub>16</sub>O<sub>2</sub>, C<sub>12</sub>H<sub>24</sub>O<sub>2</sub>, C<sub>16</sub>H<sub>32</sub>O<sub>2</sub> and C<sub>18</sub>H<sub>34</sub>O<sub>2</sub>  
892 that were difficult to attribute to individual chemical species because of prevalence of  
893 several possible isomers. These isomers were most probably esters and carboxylic acids  
894 that are used in many consumer, commercial, and industrial applications. The esters  
895 could have contributed more in some cases given their higher volatility, and also because  
896 some carboxylic acids are used as feedstocks to produce esters. We briefly discuss these  
897 ions here to guide future measurements.

898

899 C<sub>7</sub>H<sub>14</sub>O<sub>2</sub> was the most abundant ion in this group likely due to contributions from amyl  
900 acetate, isoamyl acetate, and butyl propionate that are used as solvents,  
901 fragrances/flavorings, and in other commercial/industrial applications, with possible  
902 contributions from heptanoic acid. C<sub>8</sub>H<sub>16</sub>O<sub>2</sub> was the next most prominent and likely  
903 related to octanoic acid, hexyl acetate, pentyl propanoate and butyl butyrate. C<sub>8</sub>H<sub>16</sub>O<sub>2</sub>  
904 emissions ( $\sim 5 \times 10^3$  kg yr<sup>-1</sup>) were predominantly (90%) estimated to be hexyl acetate by  
905 the VCPy $\pm$  model. In comparison, amyl acetate (i.e. C<sub>7</sub>H<sub>14</sub>O<sub>2</sub>) is estimated in much  
906 smaller amounts across the two inventories ( $\sim 5$ -500 kg yr<sup>-1</sup>). Yet, the higher abundance  
907 of C<sub>7</sub>H<sub>14</sub>O<sub>2</sub> suggested major contributions from other isomers and/or variations in CI-ToF  
908 sensitivity. By comparison, we calibrated C<sub>8</sub>H<sub>16</sub>O<sub>2</sub> using octanoic acid given its  
909 widespread use in various personal care and cosmetic products. This gave C<sub>8</sub>H<sub>16</sub>O<sub>2</sub>  
910 concentrations ranging from 50 to 300 ppt across the measurement period, but  
911 considerable variation is possible with ester contributions to the ions' mass response  
912 factors. Among other ions, the abundance of C<sub>12</sub>H<sub>24</sub>O<sub>2</sub> was comparable to C<sub>8</sub>H<sub>16</sub>O<sub>2</sub>. The  
913 larger ions, C<sub>16</sub>H<sub>32</sub>O<sub>2</sub> and C<sub>18</sub>H<sub>34</sub>O<sub>2</sub> showed very small (<10 ions s<sup>-1</sup>) abundances  
914 throughout the campaign. Interestingly, the low ion abundances occurred despite the  
915 VCPy $\pm$  model's sizable emission estimates of alkyl methyl esters (C<sub>16</sub>-C<sub>18</sub>) on the order  
916 of 10<sup>5</sup> kg yr<sup>-1</sup> in NYC, which is similar to more volatile esters such as methyl or ethyl  
917 acetates. This highlights the importance of further research on these semi-volatile organic

918 compounds across seasons to examine if they have lower emissions or could have  
919 partitioned to the particle phase in the atmosphere during the winter.

920

### 921 **3.5 Assessment of ambient concentrations relative to current emissions inventories**

922 In our analysis, high emission estimates did not always translate to high average ambient  
923 concentrations and vice versa (Figures 7, [S10S12](#)), which warrants further examination of  
924 ions (and contributing isomers) that were either highly abundant, differed significantly  
925 from expected based on emissions inventories, or had limited prior measurements.

926 Though ambient concentrations of a chemical species may not always directly reflect the  
927 magnitude of its primary emissions due to atmospheric processes, relative concentrations  
928 are frequently used in studies to evaluate the relative magnitude of emissions of various  
929 compounds (Gkatzelis et al., 2021a; McDonald et al., 2018).

930

931 Figures 7a-b shows the prevalence of such ions during the sampling period relative to  
932 their estimated annual emissions against two different regionally-resolved inventories  
933 specifically for NYC. The annual emissions were calculated as the sum of the annual  
934 emissions of all isomers reported in inventories that contributed to each ion formula. ~~Both~~  
935 ~~axes in figures 7a-b are ratioed to C<sub>3</sub>H<sub>6</sub>O (predominantly acetone) since it was among the~~  
936 ~~most abundant ions measured in this study and its primary isomer, acetone, has extensive,~~  
937 ~~diverse uses in various products and materials with the majority of anthropogenic~~  
938 ~~emissions coming from VCP-related sources. Both axes in figures 7a-b are ratioed to~~  
939 ~~C<sub>3</sub>H<sub>6</sub>O (predominantly acetone) since it was among the most abundant ions measured in~~  
940 ~~this study and its primary isomer, acetone, has extensive, diverse uses in various products~~  
941 ~~and materials with the majority of anthropogenic emissions in NYC coming from VCP-~~  
942 ~~related sources (Gkatzelis et al., 2021b).~~ Still, we acknowledge that acetone, like many  
943 oxygenated compounds, could see contributions from oxidation processes. However,  
944 such secondary production would be at its minimum during this January study period,  
945 and, the short timescales of emitted compounds' transport within the urban footprint  
946 reduces (Figure S2) its potential influence in this analysis. Furthermore, to account for  
947 any regional background influence in the calculation of emission ratios for inventory  
948 comparisons, we have subtracted the estimated ambient background using ~~thea~~ 5<sup>th</sup>  
949 percentile concentration value to focus on enhancements in the urban area during the  
950 study, ~~similar to prior work~~.

951

952 We also note that choosing an ideal denominator species in the middle of a complex,  
953 dense urban environment with a wide array of spatiotemporally-dynamic sources is  
954 highly challenging. Given the varying correlation coefficients between compounds

955 (Figure 6), Table 1 and Figure 7 are presented using geometric mean ratios of  
956 concentration enhancements above the observed ambient background (i.e. 5<sup>th</sup> percentile).  
957 This enables comparisons across all measured compounds, though a comparison of  
958 concentration ratios versus slopes from least-squares regressions generally yielded  
959 comparable results for acetone for well-correlated species (Figure S11-S13), which also  
960 indicates the subtraction of average regional background to determine mean urban  
961 enhancement ratios (Table 1) was similarly effective for inventory comparisons. We note  
962 that this comparison is done with data from January in a very densely populated area and  
963 acetone concentrations will have seasonal variations from biogenic and secondary  
964 sources that should be considered in future comparisons between seasons/sites. During  
965 this 10-day period, the benzene-to-acetone ratio was close to that predicted by the VCPy<sub>±</sub>  
966 inventory, albeit with slightly greater than expected (i.e. 21.8:1) inferring additional  
967 benzene anthropogenic or biomass burning related emissions than in the inventory (see  
968 Section 2), but supports that acetone is not overestimated in the inventory when  
969 compared to a more commonly-used anthropogenic tracer (i.e. benzene).

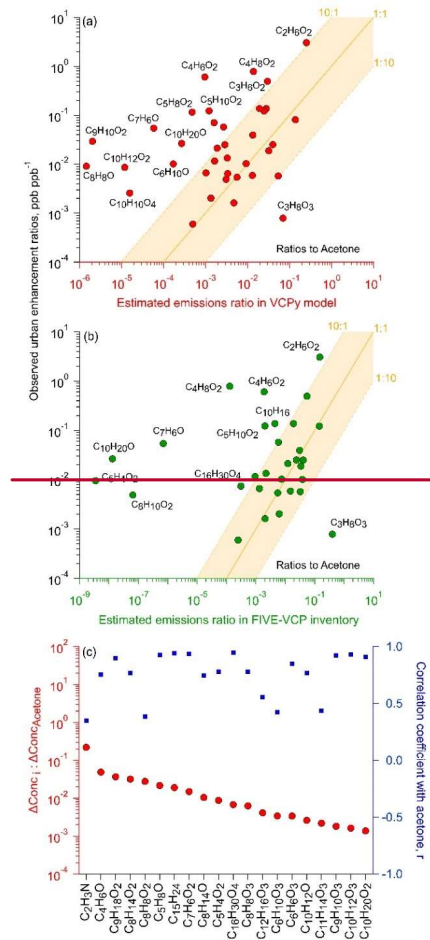
970

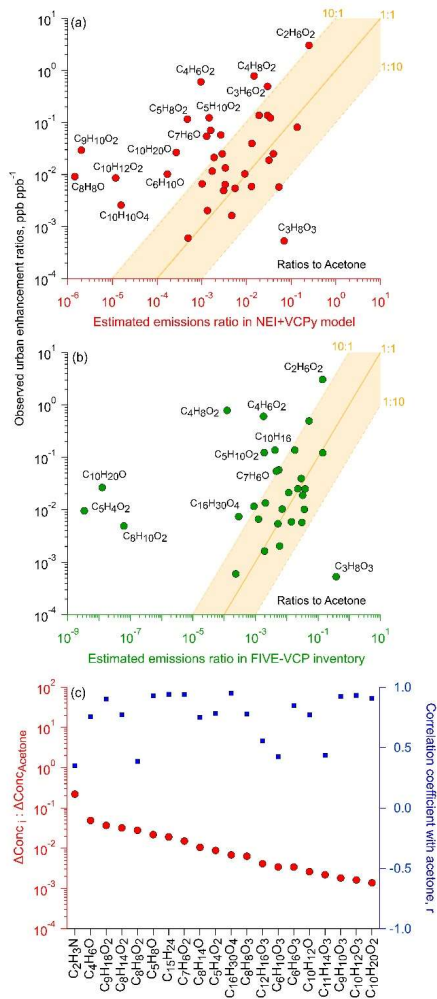
971 As common markers of anthropogenic activities, the observed ions were also compared  
972 against CO and benzene, but, acetone and benzyl alcohol had a greater number of strong  
973 correlations ( $0.9 < r < 1$ ) in this densely populated area (Figure 6, Tables 1, S5-S8).  
974 Wherever appropriate, the following discussion in this subsection also draws upon  
975 correlations with other ions that may inform source subtypes or emission pathways  
976 (Figures S12-S15-S14-S17), with more detailed discussion available in the supplemental  
977 information (SI). There was some variation in the number of speciated compounds  
978 included in each inventory and, a subset of calibrated ions in this study were not available  
979 in one of the emissions inventories. The compounds not speciated in VCPy are presented  
980 in Figure 7c with mean concentrations relative to acetone.

981

982 Of the 58 calibrated ions, emissions of one or more isomers were reported for 38 ions in  
983 VCPy<sub>±</sub> and 32 ions in FIVE-VCP inventories. The ambient concentration ratios of  
984 roughly half of these numbers agreed within 1 order of magnitude (i.e. 1:10, 10:1) with  
985 emissions reported in both inventories (Figure 7a-b). Within this sub-fraction,  
986 concentrations of 50% of ions nearly matched with estimates, though with some  
987 variability between inventories. In the case of VCPy<sub>±</sub> (Figure 7a), some of the most  
988 accurately estimated ions represented glycol and glycol ether compound categories, such  
989 as dipropylene- and triethylene- glycols, 2-butoxyethanol, 2-methoxyethanol (with  
990 propylene glycol), and phenoxyethanol, as well as D5, pentanedioic acid dimethyl ester,  
991 methyl pyrrolidone, benzyl alcohol, monoterpenes and diethyl phthalate. Several other

992 ions also representing glycols and glycol ethers fell within the 1:10 range (Figure  
993 [S16S18](#)), but not ethylene glycol (see discussion below).





996 **Figure 7. Comparison of ambient observations to emission inventories. (including all**  
997 **inventoried anthropogenic sources). Urban concentration enhancement ratios against**  
998 **acetone (calculated via background-subtracted geometric means) compared to estimated**  
999 **emission ratios using the (a) VCPy model (plus other anthropogenic sources in NEI) and (b)**  
1000 **FIVE-VCP inventory (shown for compounds with explicit estimates in each inventory, see**  
1001 **Table 1). (c) Concentration enhancement ratios against acetone (and correlation**  
1002 **coefficients) for calibrated ions where emissions data was not available in VCPy (panel a).**

1003 Note: Examples of isomers contributing to ions in (a) and (b) are listed in Tables 1 and  
1004 [S4S7](#).

1005 The ions in closest agreement with FIVE-VCP estimates shown in Figure 7b represented  
1006 benzyl alcohol, methyl pyrrolidone, MEK, D5 and a smaller number of glycol ethers that  
1007 included ethylene glycol hexyl ether, and, dipropylene- and diethylene- glycols. Other  
1008 ions within the tolerance bound included methyl- and butyl-acetates, 2-hexanone,  
1009 cyclohexanone and pentanedioic acid dimethyl ester. It is notable that ambient  
1010 measurements of glycols and glycol ethers made up approximately half of the total ions  
1011 that broadly agreed with emission estimates in both emissions inventories. Additionally,  
1012 the accuracy of benzyl alcohol estimates is also useful since ~45% of all mass calibrated  
1013 ions and ~35% of the total observed ions in this study correlated strongly ( $0.9 < r < 1.0$ )  
1014 with  $C_7H_8O$  (i.e. benzyl alcohol; Figures 6, [S17-S18](#)[S19-S20](#)), which may help in  
1015 constraining emissions in future studies.

1016

1017 The observed ambient ratios of the remaining ~50% ions deviated considerably from  
1018 those in emissions inventory estimates. The majority of these ions had greater  
1019 concentration ratios in Figure 7a-b, which suggests that their emissions were higher than  
1020 that expected based on emissions inventories. These elevated ratios above the 1:1 line  
1021 could be due to underestimates in VCP-related sources as well as uncertainties in other  
1022 sources, such as cooking (and the underlying foods/beverages), combustion-related  
1023 sources, industrial/commercial activities, humans (e.g. skin oil-related products; e.g. 6-  
1024 MHO), or other understudied non-traditional sources (e.g., building materials).  
1025 Additionally, while at its minima in peak wintertime conditions, secondary oxidation  
1026 products as a result of local chemistry (i.e. not in the regional background that was  
1027 subtracted) could make minor contributions to the calculated urban enhancements in  
1028 Table 1. Among glycols in particular, ethylene glycol was abundant with mean ambient  
1029 concentration ratios slightly over 10 times the inventory-based value. This result could be  
1030 influenced by seasonal variations in use, such as wintertime use as a de-icer for surfaces  
1031 (or aircraft) or the particularly elevated concentrations (25-35 ppb) during the first 4 days  
1032 of the measurement period (Figure 5) compared to the timeseries of other VOCs (Figure  
1033 4). with wind currents from the southwestern direction to the sampling site. However,  
1034 this concentration enhancement in ethylene glycol may not translate to other seasons due  
1035 to change in the magnitude of its sources (e.g. no de-icing required in non-winter  
1036 periods). Ethylene glycol also correlated strongly ( $r > 0.9$ ) with a few other ions (e.g.  
1037 MEK, MVK, cyclopentanone, cyclohexanone, benzyl alcohol) that may suggest a mix of  
1038 co-located and/or shared source types. Among glycol ethers, the  $C_8H_{10}O_2$  ion  
1039 representing phenoxyethanol differed considerably between the two inventories, ranging  
1040 from near expected in VCPy $^+$  to a much higher ambient abundance relative to FIVE-  
1041 VCP (Figure [S16](#)[S18](#)). This was likely due to estimated phenoxyethanol emissions being

1042  $10^5$  times higher in VCPy $\pm$  than in FIVE-VCP. However, 1,4-dimethoxybenzene might  
1043 have also contributed to C<sub>8</sub>H<sub>10</sub>O<sub>2</sub> ion signal given its widespread use in personal care  
1044 products but needs inclusion in emissions inventories. Similarly, monoterpenes during  
1045 this study slightly exceeded the 10:1 value based on FIVE-VCP estimates (Figure 7),  
1046 which was influenced by significantly different limonene emissions between the two  
1047 inventories (60206 kg yr<sup>-1</sup>; VCPy vs 17107 kg yr<sup>-1</sup>; FIVE-VCP) that constituted over  
1048 90% of the reported monoterpene emissions. D4-siloxane deviated in the other direction  
1049 going from near expected in FIVE-VCP to considerably above the 10:1 bound in VCPy  
1050 comparisons, which was likely due to a factor of 8 difference in its reported emissions  
1051 between the two inventories. The cyclohexanone-related C<sub>6</sub>H<sub>10</sub>O concentration ratio was  
1052 somewhat lower than expected based on FIVE-VCP estimates though within the lower  
1053 tolerance bound, but substantially exceeded VCPy $\pm$  estimates (Figure S16S18) given the  
1054 ~280-fold difference in cyclohexanone emissions between the two inventories.

1055

1056 Some ions deviated even more substantially in ambient concentration ratios relative to  
1057 inventory-based expectations (Figure 7a). The prominent ions in this group represented  
1058 esters, e.g. C<sub>9</sub>H<sub>10</sub>O<sub>2</sub> (e.g. benzyl acetate), C<sub>4</sub>H<sub>6</sub>O<sub>2</sub> (e.g. methyl acrylate), C<sub>5</sub>H<sub>8</sub>O<sub>2</sub> (e.g.  
1059 MMA), C<sub>5</sub>H<sub>10</sub>O<sub>2</sub> (e.g. isopropyl acetate) and C<sub>4</sub>H<sub>8</sub>O<sub>2</sub> (e.g. ethyl acetate). All these  
1060 compounds (except MMA) are found in solvents, fragrances, food flavorings, and  
1061 naturally in some food (e.g. fruits). Some fraction of their discrepancies may be attributed  
1062 to uncertain fragrances source categories in emissions inventories which contributes, in  
1063 part, to their higher than expected concentrations in our analysis. Hence, further work is  
1064 needed to more comprehensively speciate and constrain synthetic and natural fragrance-  
1065 related emissions. Other possibilities for these differences include missing sources that  
1066 need to be accounted for in estimating total emissions for each ion. For example, diacetyl  
1067 is also a likely isomer of C<sub>4</sub>H<sub>6</sub>O<sub>2</sub> that is currently excluded from emissions inventories.  
1068 MMA concentrations at 100's of parts per trillion (Figure 5) is an interesting case due to  
1069 its minimal use in consumer products, and, besides contributions from other isomers to  
1070 C<sub>5</sub>H<sub>8</sub>O<sub>2</sub> ion, may indicate ambient observations of PMMA offgassing/degradation under  
1071 ambient conditions. Similarly, higher than expected C<sub>10</sub>H<sub>10</sub>O<sub>4</sub> (e.g. dimethyl phthalate)  
1072 concentrations could be contributed to by materials-related off-gassing and emissions  
1073 from personal care products.

1074

1075 Ions related to benzaldehyde and menthol also exhibited higher than expected  
1076 concentrations in both inventory assessments. C<sub>10</sub>H<sub>20</sub>O (e.g. menthol) showed strong  
1077 correlations ( $r > 0.95$ ) with 14 other ions that spanned several compound classes  
1078 including glycol ethers, carbonyls, esters and alcohol. This may be also contributed to by  
1079 fragrance-related sources, or other isomers in the case of menthol. C<sub>9</sub>H<sub>10</sub>O<sub>2</sub> (e.g. benzyl

1080 acetate), C<sub>10</sub>H<sub>12</sub>O<sub>2</sub> (e.g. eugenol) and C<sub>6</sub>H<sub>10</sub>O (e.g. cyclohexanone) ions also showed high  
1081 concentrations in VCPy<sub>±</sub> inventory comparisons while C<sub>5</sub>H<sub>4</sub>O<sub>2</sub> (e.g. furfural) exceeded  
1082 expected concentrations based on FIVE-VCP estimates. Furfural could also be  
1083 contributed by indoor emissions from wood-based materials (Sheu et al., 2021) though  
1084 such a source will be lower in NYC than observed elsewhere given major differences in  
1085 Manhattan building construction materials. Some of these isomers, e.g. eugenol,  
1086 raspberry ketone and furfural ~~are~~ also appear in foods and ~~are~~ used in ~~fo~~odas flavorings,  
1087 which remains largely unexplored as a potential source of emissions.

1088

1089 The glycerol-related C<sub>3</sub>H<sub>8</sub>O<sub>3</sub> ion presents a very interesting case among the few ions that  
1090 exhibited considerably lower concentrations than expected, with regional background  
1091 concentrations even dropping below its detection limit (see Table S5). Its annual  
1092 estimated emissions are comparable to prominent carbonyls and esters with slight  
1093 differences between the VCPy<sub>±</sub> and FIVE-VCP inventories ( $\sim 10^5$  kg yr<sup>-1</sup> vs.  $\sim 10^6$  kg yr<sup>-1</sup>).  
1094 However, it is uncertain whether its low mean concentration during the sampling  
1095 period (Table 1) was influenced by seasonal variations in ambient gas-to-particle  
1096 partitioning and/or in emissions pathways (e.g. reduced evaporation or indoor-to-outdoor  
1097 transport). Thus, further research would be valuable to evaluate atmospheric levels of  
1098 glycerol including during summertime conditions when evaporative emissions from  
1099 personal care products and indoor-to-outdoor transport are enhanced relative to January.  
1100 The same factors may have also driven the somewhat lower concentrations of texanol  
1101 relative to inventory-based predictions (Figures 7a-b, SI6S18), though its concentrations  
1102 are similar to summertime observations in NYC (Stockwell et al., 2021).

1103

1104 Among ions without any emissions estimates, C<sub>8</sub>H<sub>8</sub>O<sub>2</sub> (e.g. methyl benzoate), C<sub>9</sub>H<sub>18</sub>O<sub>2</sub>  
1105 (e.g. heptyl acetate) and C<sub>7</sub>H<sub>6</sub>O<sub>2</sub> (e.g. benzoic acid) had some of the highest  
1106 concentration ratios to acetone (Figure 7c), and may warrant inclusion in emission  
1107 inventories, potentially as part of “fragrances” or other uncertain source types.  
1108 Observations of sesquiterpenes were 7% of acetone concentrations on average (Table 1).  
1109 The mean sesquiterpenes to monoterpenes ratio was  $\sim 0.5$  during the measurement period  
1110 though sensitive to instrument calibration, emphasizing sizable contributions from the  
1111 highly-reactive sesquiterpenes to urban air. Ions including C<sub>4</sub>H<sub>6</sub>O (e.g. MVK), C<sub>8</sub>H<sub>14</sub>O<sub>2</sub>  
1112 (e.g. cyclohexyl acetate), C<sub>5</sub>H<sub>8</sub>O (e.g. cyclopentanone) and C<sub>8</sub>H<sub>14</sub>O (e.g. 6-methyl-5-  
1113 hepten-2-one, a skin oil oxidation product) were not estimated in the inventory, but  
1114 showed very strong correlations ( $0.9 < r < 1.0$ ) with the acetone-related C<sub>3</sub>H<sub>6</sub>O ion.

1115

1116 **4. Conclusions and future work**

1117 A Vocus CI-ToF using low-pressure NH<sub>4</sub><sup>+</sup> as the reagent ion enabled measurements of a  
1118 wide range of oxygenated species in New York City whose urban enhancements were  
1119 primarily attributed to anthropogenic sources given the peak wintertime conditions, but  
1120 could vary under different meteorological conditions. Our results highlight the diversity  
1121 of oxygenated compounds in urban air, including VCP-related compounds that extend  
1122 considerably beyond the highly volatile, functionalized species found in oxygenated  
1123 solvents. The measured ions had contributions from VOCs to I/SVOCs including  
1124 acetates, glycols, glycol ethers, alcohols, acrylates and other functional groups. The  
1125 atmospheric concentrations of these species varied over a large range but reached up to  
1126 hundreds of ppt and into ppb-levels in several cases, which were comparable to the  
1127 prevalence of known prominent OVOCs such as acetone, MEK and MVK. While  
1128 emissions inventories predicted the relative abundance of many species in the atmosphere  
1129 with relative accuracy (e.g. glycols and glycol ethers), several others deviatedshowed  
1130 significantly different ambient concentrations than predicted (e.g. select esters). This  
1131 informs measured over 10 times their expected values (Figure 7).

1132 While the species target list in this manuscript (Table 1) included an array of compounds  
1133 that are known to occur in VCPs, the observed underestimates when compared to  
1134 emission inventories may be contributed to not only VCP-related sources but also other  
1135 established or uncertain urban sources in the inventories. Broad source classes such as  
1136 cooking (and associated foods/fuels) represent one example that could be significant  
1137 sources of some of the OVOCs studied here (e.g., esters, carbonyls, fatty acids,  
1138 terpenoids). Similarly, while large biomass burning influences were filtered from the  
1139 comparison to the emission inventories, we note that biomass burning remains an  
1140 important source of regional and/or long-distance OVOCs. Regional and long-distance  
1141 transport of secondary OVOCs (and associated pollutants) also remain important  
1142 contributors to urban air quality across all seasons, and non-wintertime conditions will  
1143 include a greater role for photochemical processing within/near NYC. Yet, local  
1144 secondary OVOCs can be produced within the city, and future work with longer NH4+  
1145 based summertime datasets can further deconvolve OVOC contributions, including the  
1146 contributions of local photochemical production (occurring from outdoor or indoor  
1147 chemistry).

1148 These results inform new avenues for investigation of investigating the emissions or  
1149 atmospheric dynamics of these species indoors or outdoors, and possible additional  
1150 compounds and source contributions for inclusion in emissions inventories. Given the  
1151 high ambient prevalence of some species, further research is also warranted to further  
1152 enhance chemical speciation in inventories (and measurements) that will constrain  
1153 potential contributions to SOA and ozone formation under varying environmental  
1154 conditions. Future summertime studies (e.g. **AEROMMA, GOTHAAM**) will also provide  
1155 valuable opportunities to compare seasonal abundances of observed species and to study

1156 different seasonally-dependent emission pathways: [Atmospheric Emissions and Reactions](#)  
1157 [Observed from Megacities to Marine Areas \(AEROMMA\) \(Warneke et al., 2022\)](#),  
1158 [Greater New York Oxidant, Trace gas, Halogen and Aerosol Airborne Mission](#)  
1159 [\(GOTHAAM\)](#) will also provide valuable opportunities to compare seasonal abundances  
1160 [of observed species and to study different seasonally-dependent emission pathways.](#)

1161

## 1162 **Author Contributions**

1163 D.R.G., J.E.M. (SBU), and J.E.K. conceived the study, and J.E.K. performed the ambient  
1164 Vocus CI-ToF measurements with support from R.T.C. P.K. led data analysis and writing  
1165 with support from J.E.K and D.R.G., and contributions/review from other co-authors.  
1166 P.K., J.E.M. (Yale) and J.W. prepared calibration mixes. J.E.M. (Yale), J.W. and J.E.K  
1167 performed in-lab calibrations. T.H.M. collected EI-MS samples and conducted related  
1168 analysis, along with J.W. and J.E.M. (Yale). K.M.S and H.O.T.P. developed the VCPy  
1169 model and K.M.S. performed VCPy calculations for this work. B.M. provided the FIVE-  
1170 VCP emissions inventory data used in this study. F.M. and F.L.H. developed and tested  
1171 the Vocus CI-ToF instrument for this study. C.C. and J.E.M. (SBU) performed PTR-ToF  
1172 measurements used for instrument cross-validation in this study. R.C. provided carbon  
1173 monoxide data and R.T.C. helped setting up the measurement site.

1174

## 1175 **Competing interests**

1176 Jordan E. Krechmer is employed by Aerodyne Research, Inc., which commercializes the  
1177 Vocus CI-ToF instrument for geoscience research and Felipe Lopez-Hilfiker is an  
1178 employee of Tofwerk, AG, which manufactures and sells the Vocus CI-ToF instrument  
1179 used in this study.

1180

## 1181 **Acknowledgements**

1182 We thank the Northeast States for Coordinated Air Use Management (NESCAUM) for  
1183 funding this research through a contract with the New York State Energy Research and  
1184 Development Authority (NYSERDA) (Agreement No. 101132) as part of the LISTOS  
1185 project. Any opinions expressed in this article do not necessarily reflect those of  
1186 NYSERDA or the State of New York. We also would like to acknowledge financial  
1187 support from U.S. NSF (CBET-2011362 and AGS-1764126), and Columbia University.  
1188 We thank the City University of New York for facilitating sampling at their Advanced  
1189 Science Research Center. The views expressed in this article are those of the authors and  
1190 do not necessarily represent the views or policies of the U.S. Environmental Protection  
1191 Agency.

1192

1193 **References**

1194 [Abbatt, J. P. D. and Wang, C.: The atmospheric chemistry of indoor environments,](#)  
1195 [Environ. Sci. Process. Impacts, 22\(1\), 25–48, doi:10.1039/C9EM00386J, 2020.](#)

1196 [Anon: U.S. Environmental Protection Agency, Chemical Data Reporting 2016, \[online\]](#)  
1197 Available from: <https://www.epa.gov/chemical-data-reporting/access-cdr-data>, 2016.

1198 Asaf, D., Tas, E., Pedersen, D., Peleg, M. and Luria, M.: Long-Term Measurements of  
1199 NO<sub>3</sub> Radical at a Semiarid Urban Site: 2. Seasonal Trends and Loss Mechanisms,  
1200 Environ. Sci. Technol. , 44, 5901–5907, doi:10.1021/es100967z, 2010.

1201 Aschmann, S. M., Martin, P., Tuazon, E. C., Arey, J. and Atkinson, R.: Kinetic and  
1202 product studies of the reactions of selected glycol ethers with OH radicals, Environ. Sci.  
1203 Technol., 35(20), 4080–4088,  
1204 doi:10.1021/ES010831K/SUPPL\_FILE/ES010831K\_S.PDF, 2001.

1205 Bennet, F., Hart-Smith, G., Gruendling, T., Davis, T. P., Barker, P. J. and Barner-  
1206 Kowollik, C.: Degradation of poly(methyl methacrylate) model compounds under  
1207 extreme environmental conditions, Macromol. Chem. Phys., 211(13), 1083–1097, 2010.

1208 Bi, C., Liang, Y. and Xu, Y.: Fate and Transport of Phthalates in Indoor Environments  
1209 and the Influence of Temperature: A Case Study in a Test House, Environ. Sci. Technol.,  
1210 49(16), 9674–9681, doi:10.1021/acs.est.5b02787, 2015.

1211 Bi, C., Krechmer, J. E., Frazier, G. O., Xu, W., Lambe, A. T., Claflin, M. S., Lerner, B.  
1212 M., Jayne, J. T., Worsnop, D. R., Canagaratna, M. R. and Isaacman-Vanwertz, G.:  
1213 Quantification of isomer-resolved iodide chemical ionization mass spectrometry  
1214 sensitivity and uncertainty using a voltage-scanning approach, Atmos. Meas. Tech.,  
1215 14(10), 6835–6850, doi:10.5194/AMT-14-6835-2021, 2021.

1216 Bornehag, C. G., Lundgren, B., Weschler, C. J., Sigsgaard, T., Hagerhed-Engman, L. and  
1217 Sundell, J.: Phthalates in indoor dust and their association with building characteristics,  
1218 Environ. Health Perspect., 113(10), 1399–1404, doi:10.1289/ehp.7809, 2005.

1219 Canaval, E., Hyttinen, N., Schmidbauer, B., Fischer, L. and Hansel, A.: NH<sub>4</sub><sup>+</sup>  
1220 association and proton transfer reactions with a series of organic molecules, Front.  
1221 Chem., 7(APR), 191, doi:10.3389/FCHEM.2019.00191/BIBTEX, 2019.

1222 Cao, H., Li, X., He, M. and Zhao, X. S.: Computational study on the mechanism and  
1223 kinetics of NO<sub>3</sub>-initiated atmosphere oxidation of vinyl acetate, Comput. Theor. Chem.,  
1224 1144, 18–25, doi:10.1016/J.COMPTC.2018.09.012, 2018.

1225 Charan, S. M., Buenconsejo, R. S. and Seinfeld, J. H.: Secondary organic aerosol yields  
1226 from the oxidation of benzyl alcohol, Atmos. Chem. Phys., 20(21), 13167–13190,  
1227 doi:10.5194/ACP-20-13167-2020, 2020.

1228 Choi, H., Schmidbauer, N., Sundell, J., Hasselgren, M., Spengler, J. and Bornehag, C. G.:  
1229 Common household chemicals and the allergy risks in pre-school age children, PLoS  
1230 One, 5(10), doi:10.1371/journal.pone.0013423, 2010a.

1231 Choi, H., Schmidbauer, N., Spengler, J. and Bornehag, C. G.: Sources of propylene  
1232 glycol and glycol ethers in air at home, *Int. J. Environ. Res. Public Health*, 7(12), 4213–  
1233 4237, doi:10.3390/ijerph7124213, 2010b.

1234 Coggon, M. M., McDonald, B. C., Vlasenko, A., Veres, P. R., Bernard, F., Koss, A. R.,  
1235 Yuan, B., Gilman, J. B., Peischl, J., Aikin, K. C., Durant, J., Warneke, C., Li, S. M. and  
1236 De Gouw, J. A.: Diurnal Variability and Emission Pattern of  
1237 Decamethylcyclopentasiloxane (D5) from the Application of Personal Care Products in  
1238 Two North American Cities, *Environ. Sci. Technol.*, 52(10), 5610–5618,  
1239 doi:10.1021/acs.est.8b00506, 2018.

1240 Coggon, M. M., Gkatzelis, G. I., McDonald, B. C., Gilman, J. B., Schwantes, R. H.,  
1241 Abuhaman, N., Aikin, K. C., Arendt, M. F., Berkoff, T. A., Brown, S. S., Campos, T. L.,  
1242 Dickerson, R. R., Gronoff, G., Hurley, J. F., Isaacman-Vanwertz, G., Koss, A. R., Li, M.,  
1243 McKeen, S. A., Moshary, F., Peischl, J., Pospisilova, V., Ren, X., Wilson, A., Wu, Y.,  
1244 Trainer, M. and Warneke, C.: Volatile chemical product emissions enhance ozone and  
1245 modulate urban chemistry, *Proc. Natl. Acad. Sci. U. S. A.*, 118(32),  
1246 doi:10.1073/PNAS.2026653118/SUPPL\_FILE/PNAS.2026653118.SAPP.PDF, 2021.

1247 Coggon, M. M., Gkatzelis, G. I., McDonald, B. C., Gilman, J. B., Schwantes, R. H.,  
1248 Abuhaman, N., Aikin, K. C., Arendt, M. F., Berkoff, T. A., Brown, S. S., Campos, T. L.,  
1249 Dickerson, R. R., Gronoff, G., Hurley, J. F., Isaacman-Vanwertz, G., Koss, A. R., Li, M.,  
1250 McKeen, S. A., Moshary, F., Peischl, J., Pospisilova, V., Ren, X., Wilson, A., Wu, Y.,  
1251 Trainer, M. and Warneke, C.: Volatile chemical product emissions enhance ozone and  
1252 modulate urban chemistry, *Proc. Natl. Acad. Sci. U. S. A.*, 118(32),  
1253 doi:10.1073/PNAS.2026653118/SUPPL\_FILE/PNAS.2026653118.SAPP.PDF, 2021.

1254 Council of the European Union: EU Directive 1999/13/EC: Reducing the emissions of  
1255 volatile organic compounds (VOCs). [online] Available from: [eur-lex.europa.eu/legal-content/EN/TXT/?uri=celex:31999L0013](http://eur-lex.europa.eu/legal-content/EN/TXT/?uri=celex:31999L0013), 1999.

1257 Destaillats, H., Lunden, M. M., Singer, B. C., Coleman, B. K., Hodgson, A. T., Weschler,  
1258 C. J. and Nazaroff, W. W.: Indoor Secondary Pollutants from Household Product  
1259 Emissions in the Presence of Ozone: A Bench-Scale Chamber Study, *Environ. Sci.  
1260 Technol.*, 40, 4421–4428, doi:10.1021/ES052198Z, 2006.

1261 Even, M., Girard, M., Rich, A., Hutzler, C. and Luch, A.: Emissions of VOCs From  
1262 Polymer-Based Consumer Products: From Emission Data of Real Samples to the  
1263 Assessment of Inhalation Exposure, *Front. Public Heal.*, 7, 202,  
1264 doi:10.3389/fpubh.2019.00202, 2019.

1265 Even, M., Hutzler, C., Wilke, O. and Luch, A.: Emissions of volatile organic compounds  
1266 from polymer-based consumer products: Comparison of three emission chamber sizes,  
1267 *Indoor Air*, 30(1), 40–48, doi:10.1111/ina.12605, 2020.

1268 Franco, B., Blumenstock, T., Cho, C., Clarisse, L., Clerbaux, C., Coheur, P. F., De  
1269 Mazière, M., De Smedt, I., Dorn, H. P., Emmerichs, T., Fuchs, H., Gkatzelis, G., Griffith,  
1270 D. W. T., Gromov, S., Hannigan, J. W., Hase, F., Hohaus, T., Jones, N., Kerkweg, A.,  
1271 Kiendler-Scharr, A., Lutsch, E., Mahieu, E., Novelli, A., Ortega, I., Paton-Walsh, C.,  
1272 Pommier, M., Pozzer, A., Reimer, D., Rosanka, S., Sander, R., Schneider, M., Strong, K.,

1273 Tillmann, R., Van Rozendaal, M., Vereecken, L., Vigouroux, C., Wahner, A. and  
1274 Taraborrelli, D.: Ubiquitous atmospheric production of organic acids mediated by cloud  
1275 droplets, *Nat. 2021* 593(7858), 233–237, doi:10.1038/s41586-021-03462-x,  
1276 2021.

1277 Gkatzelis, G. I., Coggon, M. M., McDonald, B. C., Peischl, J., Aikin, K. C., Gilman, J.  
1278 B., Trainer, M. and Warneke, C.: Identifying Volatile Chemical Product Tracer  
1279 Compounds in U.S. Cities, *Environ. Sci. Technol.*, 55(1), 188–199,  
1280 doi:10.1021/ACS.EST.0C05467/SUPPL\_FILE/ES0C05467\_SI\_001.PDF, 2021a.

1281 Gkatzelis, G. I., Coggon, M. M., McDonald, B. C., Peischl, J., Gilman, J. B., Aikin, K.  
1282 C., Robinson, M. A., Canonaco, F., Prevot, A. S. H., Trainer, M. and Warneke, C.:  
1283 Observations Confirm that Volatile Chemical Products Are a Major Source of  
1284 Petrochemical Emissions in U.S. Cities, *Environ. Sci. Technol.*, 55(8), 4332–4343,  
1285 doi:10.1021/ACS.EST.0C05471/SUPPL\_FILE/ES0C05471\_SI\_001.PDF, 2021b.

1286 de Gouw, J. A., Gilman, J. B., Kim, S. W., Lerner, B. M., Isaacman-VanWertz, G.,  
1287 McDonald, B. C., Warneke, C., Kuster, W. C., Lefer, B. L., Griffith, S. M., Dusanter, S.,  
1288 Stevens, P. S. and Stutz, J.: Chemistry of Volatile Organic Compounds in the Los  
1289 Angeles basin: Nighttime Removal of Alkenes and Determination of Emission Ratios, *J.*  
1290 *Geophys. Res. Atmos.*, 122(21), 11,843–11,861, doi:10.1002/2017JD027459, 2017.

1291 Harb, P., Locoge, N. and Thevenet, F.: Treatment of household product emissions in  
1292 indoor air: Real scale assessment of the removal processes, *Chem. Eng. J.*, 380, 122525,  
1293 doi:10.1016/j.cej.2019.122525, 2020.

1294 Heald, C. L. and Kroll, J. H.: The fuel of atmospheric chemistry: Toward a complete  
1295 description of reactive organic carbon, *Sci. Adv.*, 6(6), eaay8967,  
1296 doi:10.1126/sciadv.aay8967, 2020.

1297 Henze, D. K., Seinfeld, J. H., Ng, N. L., Kroll, J. H., Fu, T. M., Jacob, D. J. and Heald, C.  
1298 L.: Global modeling of secondary organic aerosol formation from aromatic  
1299 hydrocarbons: High- vs. low-yield pathways, *Atmos. Chem. Phys.*, 8(9), 2405–2421,  
1300 doi:10.5194/ACP-8-2405-2008, 2008.

1301 [Holzinger, R., Joe Acton, W. F., Bloss, W. W., Breitenlechner, M., Crilley, L. L.,](#)  
1302 [Dusanter, S., Gonin, M., Gros, V., Keutsch, F. F., Kiendler-Scharr, A., Kramer, L. L.,](#)  
1303 [Krechmer, J. J., Languille, B., Locoge, N., Lopez-Hilfiker, F., Materi, D., Moreno, S.,](#)  
1304 [Nemitz, E., Quéléver, L. L., Sarda Esteve, R., Sauvage, S., Schallhart, S., Sommariva, R.,](#)  
1305 [Tillmann, R., Wedel, S., Worton, D. D., Xu, K. and Zaytsev, A.: Validity and limitations](#)  
1306 [of simple reaction kinetics to calculate concentrations of organic compounds from ion](#)  
1307 [counts in PTR-MS, \*Atmos. Meas. Tech.\*, 12\(11\), 6193–6208, doi:10.5194/AMT-12-](#)  
1308 [6193-2019, 2019.](#)

1309 [Huangfu, Y., Yuan, B., Wang, S., Wu, C., He, X., Qi, J., de Gouw, J., Warneke, C.,](#)  
1310 [Gilman, J. B., Wisthaler, A., Karl, T., Graus, M., Jobson, B. T. and Shao, M.: Revisiting](#)  
1311 [Acetonitrile as Tracer of Biomass Burning in Anthropogenic-Influenced Environments,](#)  
1312 [\*Geophys. Res. Lett.\*, 48\(11\), e2020GL092322, doi:10.1029/2020GL092322, 2021.](#)

1313 Humes, M. B., Wang, M., Kim, S., Machesky, J. E., Gentner, D. R., Robinson, A. L.,

1314 Donahue, N. M. and Presto, A. A.: Limited Secondary Organic Aerosol Production from  
1315 Acyclic Oxygenated Volatile Chemical Products, *Environ. Sci. Technol.*, 56(8), 4806–  
1316 4815, doi:10.1021/acs.est.1c07354, 2022.

1317 Karl, T., Striednig, M., Graus, M., Hammerle, A. and Wohlfahrt, G.: Urban flux  
1318 measurements reveal a large pool of oxygenated volatile organic compound emissions, ,  
1319 115(6), 1186–1191, doi:10.1073/pnas.1714715115, 2018.

1320 Khare, P. and Gentner, D. R.: Considering the future of anthropogenic gas-phase organic  
1321 compound emissions and the increasing influence of non-combustion sources on urban  
1322 air quality, *Atmos. Chem. Phys.*, 18(8), doi:10.5194/acp-18-5391-2018, 2018.

1323 Khare, P., Machesky, J., Soto, R., He, M., Presto, A. A. and Gentner, D. R.: Asphalt-  
1324 related emissions are a major missing nontraditional source of secondary organic aerosol  
1325 precursors, *Sci. Adv.*, 6(36), eabb9785, 2020.

1326 [Koss, A. R., Sekimoto, K., Gilman, J. B., Selimovic, V., Coggon, M. M., Zarzana, K. J.,](#)  
1327 [Yuan, B., Lerner, B. M., Brown, S. S., Jimenez, J. L., Krechmer, J., Roberts, J. M.,](#)  
1328 [Warneke, C., Yokelson, R. J. and De Gouw, J.: Non-methane organic gas emissions from](#)  
1329 [biomass burning: Identification, quantification, and emission factors from PTR-ToF](#)  
1330 [during the FIREX 2016 laboratory experiment, Atmos. Chem. Phys.](#), 18(5), 3299–3319,  
1331 doi:10.5194/ACP-18-3299-2018, 2018.

1332 Krechmer, J., Lopez-Hilfiker, F., Koss, A., Hutterli, M., Stoermer, C., Deming, B.,  
1333 Kimmel, J., Warneke, C., Holzinger, R., Jayne, J., Worsnop, D., Fuhrer, K., Gonin, M.  
1334 and De Gouw, J.: Evaluation of a New Reagent-Ion Source and Focusing Ion–Molecule  
1335 Reactor for Use in Proton-Transfer-Reaction Mass Spectrometry, , 90(20), 12011–12018,  
1336 doi:10.1021/acs.analchem.8b02641, 2018.

1337 Krechmer, J. E., Pagonis, D., Ziemann, P. J. and Jimenez, J. L.: Quantification of Gas-  
1338 Wall Partitioning in Teflon Environmental Chambers Using Rapid Bursts of Low-  
1339 Volatility Oxidized Species Generated in Situ, *Environ. Sci. Technol.*, 50(11), 5757–  
1340 5765, doi:10.1021/acs.est.6b00606, 2016.

1341 Li, W., Li, L., Chen, C. li, Kacarab, M., Peng, W., Price, D., Xu, J. and Cocker, D. R.:  
1342 Potential of select intermediate-volatility organic compounds and consumer products for  
1343 secondary organic aerosol and ozone formation under relevant urban conditions, *Atmos.*  
1344 *Environ.*, 178, 109–117, doi:10.1016/J.ATMOSENV.2017.12.019, 2018.

1345 Liang, Y., Caillot, O., Zhang, J., Zhu, J. and Xu, Y.: Large-scale chamber investigation  
1346 and simulation of phthalate emissions from vinyl flooring, *Build. Environ.*, 89, 141–149,  
1347 doi:10.1016/j.buildenv.2015.02.022, 2015.

1348 Mansouri, K., Grulke, C. M., Judson, R. S. and Williams, A. J.: OPERA models for  
1349 predicting physicochemical properties and environmental fate endpoints, *J. Cheminform.*,  
1350 10(1), 1–19, doi:10.1186/S13321-018-0263-1/FIGURES/1, 2018.

1351 Markowicz, P. and Larsson, L.: Influence of relative humidity on VOC concentrations in  
1352 indoor air, *Environ. Sci. Pollut. Res.*, 22(8), 5772–5779, doi:10.1007/s11356-014-3678-x,  
1353 2015.

1354 Masuck, I., Hutzler, C., Jann, O. and Luch, A.: Inhalation exposure of children to  
1355 fragrances present in scented toys, *Indoor Air*, 21(6), 501–511, doi:10.1111/j.1600-  
1356 0668.2011.00727.x, 2011.

1357 Mcdonald, B. C., De Gouw, J. A., Gilman, J. B., Jathar, S. H., Akherati, A., Cappa, C. D.,  
1358 Jimenez, J. L., Lee-Taylor, J., Hayes, P. L., McKeen, S. A., Cui, Y. Y., Kim, S.-W.,  
1359 Gentner, D. R., Isaacman-Vanwertz, G., Goldstein, A. H., Harley, R. A., Frost, G. J.,  
1360 Roberts, J. M., Ryerson, T. B. and Trainer, M.: Volatile chemical products emerging as  
1361 largest petrochemical source of urban organic emissions, *Science* (80-. ), 359(6377),  
1362 760–764 [online] Available from:  
1363 <http://science.sciencemag.org/content/sci/359/6377/760.full.pdf> (Accessed 25 February  
1364 2018), 2018.

1365 McLachlan, M. S., Kierkegaard, A., Hansen, K. M., Van Egmond, R., Christensen, J. H.  
1366 and Skjøth, C. A.: Concentrations and fate of decamethylcyclopentasiloxane (D5) in the  
1367 atmosphere, *Environ. Sci. Technol.*, 44(14), 5365–5370, doi:10.1021/es100411w, 2010.

1368 Mellouki, A., Wallington, T. J. and Chen, J.: Atmospheric Chemistry of Oxygenated  
1369 Volatile Organic Compounds: Impacts on Air Quality and Climate, *Chem. Rev.*, 115(10),  
1370 3984–4014,  
1371 doi:10.1021/CR500549N/ASSET/IMAGES/CR500549N.SOCIAL.JPG\_V03, 2015.

1372 Noguchi, M. and Yamasaki, A.: Volatile and semivolatile organic compound emissions  
1373 from polymers used in commercial products during thermal degradation, *Heliyon*, 6(3),  
1374 e03314, doi:10.1016/j.heliyon.2020.e03314, 2020.

1375 Pagonis, D., Krechmer, J. E., De Gouw, J., Jimenez, J. L. and Ziemann, P. J.: Effects of  
1376 gas–wall partitioning in Teflon tubing and instrumentation on time-resolved  
1377 measurements of gas-phase organic compounds, *Atmos. Meas. Tech.*, 10, 4687–4696,  
1378 doi:10.5194/amt-10-4687-2017, 2017.

1379 Pennington, E. A., Seltzer, K. M., Murphy, B. N., Qin, M., Seinfeld, J. H. and Pye, H. O.  
1380 T.: Modeling secondary organic aerosol formation from volatile chemical products,  
1381 *Atmos. Chem. Phys.*, 21(24), 18247–18261, doi:10.5194/ACP-21-18247-2021, 2021.

1382 Picquet-Varrault, B., Doussin, J. F., Durand-Jolibois, R., Pirali, O., Carlier, P. and  
1383 Fittschen, C.: Kinetic and Mechanistic Study of the Atmospheric Oxidation by OH  
1384 Radicals of Allyl Acetate, *Environ. Sci. Technol.*, 36(19), 4081–4086,  
1385 doi:10.1021/ES0200138, 2002.

1386 Pye, H. O. T., Ward-Caviness, C. K., Murphy, B. N., Appel, K. W. and Seltzer, K. M.:  
1387 Secondary organic aerosol association with cardiorespiratory disease mortality in the  
1388 United States, *Nat. Commun.*, 12(1), doi:10.1038/S41467-021-27484-1, 2021.

1389 Qin, M., Murphy, B. N., Isaacs, K. K., McDonald, B. C., Lu, Q., McKeen, S. A., Koval,  
1390 L., Robinson, A. L., Efstathiou, C., Allen, C. and Pye, H. O. T.: Criteria pollutant impacts  
1391 of volatile chemical products informed by near-field modelling, *Nat. Sustain.* 2020 42,  
1392 4(2), 129–137, doi:10.1038/s41893-020-00614-1, 2020.

1393 Ren, X., Brune, W. H., Mao, J., Mitchell, M. J., Lesher, R. L., Simpas, J. B., Metcalf, A.  
1394 R., Schwab, J. J., Cai, C., Li, Y., Demerjian, K. L., Felton, H. D., Boynton, G., Adams,

1395 A., Perry, J., He, Y., Zhou, X. and Hou, J.: Behavior of OH and HO<sub>2</sub> in the winter  
1396 atmosphere in New York City, *Atmos. Environ.*, 40(SUPPL. 2), 252–263,  
1397 doi:10.1016/J.ATMOSENV.2005.11.073, 2006.

1398 Ren, Y., El Baramoussi, E. M., Daële, V. and Mellouki, A.: Atmospheric chemistry of  
1399 ketones: Reaction of OH radicals with 2-methyl-3-pentanone, 3-methyl-2-pentanone and  
1400 4-methyl-2-pentanone, *Sci. Total Environ.*, 780,  
1401 doi:10.1016/J.SCITOTENV.2021.146249, 2021.

1402 [Robinson, M. A., Neuman, J. A., Huey, L. G., Roberts, J. M., Brown, S. S. and Veres, P.](#)  
1403 [R.: Temperature-dependent sensitivity of iodide chemical ionization mass spectrometers,](#)  
1404 [Atmos. Meas. Tech., 15, 4295–4305, doi:10.5194/amt-15-4295-2022, 2022.](#)

1405 Schroder, J. C., Campuzano-Jost, P., Day, D. A., Shah, V., Larson, K., Sommers, J. M.,  
1406 Sullivan, A. P., Campos, T., Reeves, J. M., Hills, A., Hornbrook, R. S., Blake, N. J.,  
1407 Scheuer, E., Guo, H., Fibiger, D. L., McDuffie, E. E., Hayes, P. L., Weber, R. J., Dibb, J.  
1408 E., Apel, E. C., Jaeglé, L., Brown, S. S., Thornton, J. A. and Jimenez, J. L.: Sources and  
1409 Secondary Production of Organic Aerosols in the Northeastern United States during  
1410 WINTER, *J. Geophys. Res. Atmos.*, 123(14), 7771–7796, doi:10.1029/2018JD028475,  
1411 2018.

1412 Schwarz, J., Makeš, O., Ondráček, J., Cusack, M., Talbot, N., Vodička, P., Kubelová, L.  
1413 and Ždímal, V.: Single Usage of a Kitchen Degreaser Can Alter Indoor Aerosol  
1414 Composition for Days, *Environ. Sci. Technol.*, 51(11), 5907–5912,  
1415 doi:10.1021/acs.est.6b06050, 2017.

1416 Seltzer, K. M., Pennington, E., Rao, V., Murphy, B. N., Strum, M., Isaacs, K. K., Pye, H.  
1417 O. T. and Pye, H.: Reactive organic carbon emissions from volatile chemical products,  
1418 *Atmos. Chem. Phys.*, 21, 5079–5100, doi:10.5194/acp-21-5079-2021, 2021.

1419 Seltzer, K. M., Murphy, B. N., Pennington, E. A., Allen, C., Talgo, K. and Pye, H. O. T.:  
1420 Volatile Chemical Product Enhancements to Criteria Pollutants in the United States,  
1421 *Environ. Sci. Technol.*, 56(11), 6905–6913,  
1422 doi:10.1021/ACS.EST.1C04298/SUPPL\_FILE/ES1C04298\_SI\_001.PDF, 2022.

1423 Shah, R. U., Coggon, M. M., Gkatzelis, G. I., McDonald, B. C., Tasoglou, A., Huber, H.,  
1424 Gilman, J., Warneke, C., Robinson, A. L. and Presto, A. A.: Urban Oxidation Flow  
1425 Reactor Measurements Reveal Significant Secondary Organic Aerosol Contributions  
1426 from Volatile Emissions of Emerging Importance, *Environ. Sci. Technol.*, 54(2), 714–  
1427 725, doi:10.1021/acs.est.9b06531, 2020.

1428 Sheu, R., Marcotte, A., Khare, P., Charan, S., Ditto, J. and Gentner, D. R.: Advances in  
1429 offline approaches for speciated measurements of trace gas-phase organic compounds via  
1430 an integrated sampling-to-analysis system, *J. Chromatogr. A*, 1575, 80–90,  
1431 doi:<https://doi.org/10.1016/j.chroma.2018.09.014>, 2018.

1432 Sheu, R., Stönnér, C., Ditto, J. C., Klüpfel, T., Williams, J. and Gentner, D. R.: Human  
1433 transport of thirdhand tobacco smoke: A prominent source of hazardous air pollutants  
1434 into indoor nonsmoking environments, *Sci. Adv.*, 6(10), eaay4109,  
1435 doi:10.1126/sciadv.aay4109, 2020.

1436 Sheu, R., Fortenberry, C. F., Walker, M. J., Eftekhari, A., Stönnér, C., Bakker, A.,  
1437 Peccia, J., Williams, J., Morrison, G. C., Williams, B. J. and Gentner, D. R.: Evaluating  
1438 Indoor Air Chemical Diversity, Indoor-to-Outdoor Emissions, and Surface Reservoirs  
1439 Using High-Resolution Mass Spectrometry, *Environ. Sci. Technol.*, 55(15), 10255–  
1440 10267, doi:10.1021/ACS.EST.1C01337/SUPPL\_FILE/ES1C01337\_SI\_001.PDF, 2021.

1441 Shi, S., Cao, J., Zhang, Y. and Zhao, B.: Emissions of Phthalates from Indoor Flat  
1442 Materials in Chinese Residences, *Environ. Sci. Technol.*, 52(22), 13166–13173,  
1443 doi:10.1021/acs.est.8b03580, 2018.

1444 Singer, B. C., Destaillats, H., Hodgson, A. T. and Nazaroff, W. W.: Cleaning products  
1445 and air fresheners: Emissions and resulting concentrations of glycol ethers and  
1446 terpenoids, *Indoor Air*, 16(3), 179–191, doi:10.1111/j.1600-0668.2005.00414.x, 2006.

1447 Slusher, D. L., Gregory Huey, L., Tanner, D. J., Flocke, F. M., Roberts, J. M., Huey, G.,  
1448 Tanner, D. J., Flocke, F. M. and Roberts, J. M.: A thermal dissociation–chemical  
1449 ionization mass spectrometry (TD-CIMS) technique for the simultaneous measurement of  
1450 peroxyacetyl nitrates and dinitrogen pentoxide, *J. Geophys. Res. Atmos.*, 109(D19), 19315,  
1451 doi:10.1029/2004JD004670, 2004.

1452 Stockwell, C. E., Coggon, M. M., I. Gkatzelis, G., Ortega, J., McDonald, B. C., Peischl,  
1453 J., Aikin, K., Gilman, J. B., Trainer, M. and Warneke, C.: Volatile organic compound  
1454 emissions from solvent-and water-borne coatings-compositional differences and tracer  
1455 compound identifications, *Atmos. Chem. Phys.*, 21(8), 6005–6022, doi:10.5194/ACP-21-  
1456 6005-2021, 2021.

1457 Thornton, J. a, Kercher, J. P., Riedel, T. P., Wagner, N. L., Cozic, J., Holloway, J. S.,  
1458 Dubé, W. P., Wolfe, G. M., Quinn, P. K., Middlebrook, A. M., Alexander, B. and Brown,  
1459 S. S.: A large atomic chlorine source inferred from mid-continental reactive nitrogen  
1460 chemistry., *Nature*, 464(7286), 271–274, doi:10.1038/nature08905, 2010.

1461 Venecek, M. A., Carter, W. P. L. and Kleeman, M. J.: Updating the SAPRC Maximum  
1462 Incremental Reactivity (MIR) scale for the United States from 1988 to 2010, *J. Air Waste*  
1463 *Manag. Assoc.*, 68(12), 1301–1316,  
1464 doi:10.1080/10962247.2018.1498410/SUPPL\_FILE/UAWM\_A\_1498410\_SM9019.DO  
1465 CX, 2018.

1466 Wang, C., Collins, D. B., Arata, C., Goldstein, A. H., Mattila, J. M., Farmer, D. K.,  
1467 Ampollini, L., DeCarlo, P. F., Novoselac, A., Vance, M. E., Nazaroff, W. W. and Abbatt,  
1468 J. P. D.: Surface reservoirs dominate dynamic gas-surface partitioning of many indoor air  
1469 constituents, *Sci. Adv.*, 6(8), 8973,  
1470 doi:10.1126/SCIADV.AAY8973/SUPPL\_FILE/AAY8973\_SM.PDF, 2020.

1471 Warneke, C., Schwantes, R., Veres, P., Rollins, A., Brewer, W. A., McDonald, B.,  
1472 Brown, S., Frost, G., Fahey, D., Aikin, K., Mak, J., Holden, B., Giles, D., Tom, P. ;,  
1473 Tolnet, H., Sullivan, J., Valin, L., Szykman, J., Quinn, T., Bates, T. and Russell, L.:  
1474 Atmospheric Emissions and Reactions Observed from Megacities to Marine Areas  
1475 (AEROMMA 2023), [online] Available from: <https://csl.noaa.gov/projects/aeromma/>  
1476 (Accessed 3 June 2022), n.d.2022.

1477 Wensing, M., Uhde, E. and Salthammer, T.: Plastics additives in the indoor  
1478 environment—flame retardants and plasticizers, *Sci. Total Environ.*, 339(1), 19–40,  
1479 doi:10.1016/j.scitotenv.2004.10.028, 2005.

1480 Weschler, C. J. and Nazaroff, W. W.: Semivolatile organic compounds in indoor  
1481 environments, *Atmos. Environ.*, 42(40), 9018–9040,  
1482 doi:10.1016/j.atmosenv.2008.09.052, 2008.

1483 Westmore, J. B. and Alauddin, M. M.: Ammonia chemical ionization mass spectrometry,  
1484 *Mass Spectrom. Rev.*, 5(4), 381–465, doi:10.1002/MAS.1280050403, 1986.

1485 Xu, L., Coggon, M. M., Stockwell, C. E., Gilman, J. B., Robinson, M. A., Breitenlechner,  
1486 M., Lamplugh, A., Neuman, J. A., Novak, G. A., Veres, P. R., Brown, S. S. and  
1487 Warneke, C.: A Chemical Ionization Mass Spectrometry Utilizing Ammonium Ions (NH  
1488 + 4 CIMS) for Measurements of Organic Compounds in the Atmosphere, *Aerosol Meas.*  
1489 Tech. Discuss., doi:10.5194/amt-2022-228, 2022.

1490 Zaytsev, A., Koss, A. R., Breitenlechner, M., Krechmer, J. E., Nihill, K. J., Lim, C. Y.,  
1491 Rowe, J. C., Cox, J. L., Moss, J., Roscioli, J. R., Canagaratna, M. R., Worsnop, D. R.,  
1492 Kroll, J. H. and Keutsch, F. N.: Mechanistic study of the formation of ring-retaining and  
1493 ring-opening products from the oxidation of aromatic compounds under urban  
1494 atmospheric conditions, *Atmos. Chem. Phys.*, 19(23), 15117–15129, doi:10.5194/acp-19-  
1495 15117-2019, 2019a.

1496 Zaytsev, A., Breitenlechner, M., Koss, A. R., Lim, C. Y., Rowe, J. C., Kroll, J. H. and  
1497 Keutsch, F. N.: Using collision-induced dissociation to constrain sensitivity of ammonia  
1498 chemical ionization mass spectrometry (NH<sub>4</sub><sup>+</sup> CIMS) to oxygenated volatile organic  
1499 compounds, *Atmos. Meas. Tech.*, 12(3), 1861–1870, doi:10.5194/AMT-12-1861-2019,  
1500 2019b.

